Development and analysis of a mobility-aware resource allocation algorithm based on min-max optimization for OFDMA femtocell networks

Nicholas Otieno Oyie

A thesis submitted in partial fulfilment for the degree of Master of Science in Telecommunication Engineering in the Jomo Kenyatta University of Agriculture and Technology

2015

Development and analysis of a mobility-aware resource allocation algorithm based on min-max optimization for OFDMA femtocell networks

Nicholas Otieno Oyie

A thesis submitted in partial fulfilment for the degree of Master of Science in Telecommunication Engineering in the Jomo Kenyatta University of Agriculture and Technology

2015

DECLARATION

This thesis is my original work and has not been presented for a degree in any other university.

Signature: _____ Date: _____

Oyie Nicholas Otieno

This thesis has been submitted for examination with our approval as the university supervisors:

Signature: _____ Date: _____

Dr. Philip Kibet Langat

JKUAT, Kenya

Signature: _____ Date: _____

Prof. Stephen Musyoki

TUK, Kenya

DEDICATION

This work is dedicated to my beloved family, especially, my late dad, may his soul rest in peace. Amen.

ACKNOWLEDGEMENTS

I would never have been able to finish my thesis without the guidance of my supervisors, help from friends, and support from my family.

I would like to express my deepest gratitude to my supervisors: Dr. Philip K. Langat and Prof. Stephen Musyoki for their excellent guidance, caring, patience, and invaluable support they provided throughout the research.

I must extend my gratitude to all my masters' colleagues for their encouragement and support.

I am deeply and forever obliged to my family for their love, support and encouragement throughout my entire life.

TABLE OF CONTENTS

LIST OF TABLES

LIST OF FIGURES

LIST OF APPENDICES

LIST OF ABBREVIATIONS

1G	First Generation
2G	Second Generation
3G	Third Generation
3GPP	Third Generation Partnership Project
4G	Fourth Generation
4T4R	Four Transmission Four Receiver
ACCS	Autonomous Component Carrier Selection
ACG	Amplitude Craving Greedy
AMC	Adaptive Modulation and Coding
AMPS	Advanced Mobile Phone System
AP	Access Points
BABS	Bandwidth Assignment Based on SNR
CapEX	Capital Expenses
C-DFP	Centralized-Dynamic Frequency Planning
CDS	Connected Dominating Set
CH	Cluster Head
CM	Cluster Member
CP	Cyclic Prefix
D-AMPS	Digital AMPS
DCAM	Distributed Clustering Algorithm
DL	Downlink
DRA	Distributed Random Access
DwPTS	Downlink Pilot Time Slot
E-UTRAN	Evolved Universal Terrestrial Radio Access
eNB	Evolved Node B
EPS	Evolved Packet System
FAPs	Femto Access Points
FAX	Facsimile
FCRA	Femtocell Cluster-based Resource Allocation
FDD	Frequency Division Duplexing

Gbps	Giga bits per second
GP	Guard Period
GPA	Global Prediction Algorithm
GSM	Global System for Mobile Communication
HeNB	Home eNB
IP	Integer Programming
ISI	Inter Symbol Interference
ITU	International Telecommunication Union
km	Kilometre
LAN	Local Area Network
LMMSE	Linear Minimum Mean Square Error
LP	Linear Programming
LPA	Local Prediction Algorithm
LTE	Long Term Evolution
M-FCRA	Mobility-aware Femtocell Cluster – based Resource Allocation
MAC	Media Access Control
MAI	Multiple Access Interference
MAO	Multi-user Adaptive OFDM
MCS	Modulation and Coding Scheme
MIMO	Multiple Input Multiple Output
MME	Mobility Management Entity
MMGW	Mobility Management Gateway
MS	Mobile Station
NMT	Nordic Mobile Telephone
OFDM	Orthogonal Frequency Division Multiple
OFDMA	Orthogonal Frequency Division Multiple Access
OpEX	Operational Expenses
OSC	Optimal Static Clustering
PAPR	Peak to Average Power ratio
PCI	Physical Cell Identity
PDC	Personal Digital Cellular
QAM	Quadrature Amplitude Modulation

QoS	Quality of Service
QPSK	Quadrature Phase Shift Keying
RB	Resource Block
RCG	Rate Craving Greedy
RRM	Radio Resource Management
RRU	Radio Resource Utilization
SC-FDMA	Single Carrier Frequency Division Multiple Access
SINR	Signal to Interference plus Noise Ratio
SIP	Session Initiation Protocol
SMS	Short Message Service
SNR	Signal to Noise Ratio
SON	Self-Optimizing Network
SSR	Spectrum Spatial Reuse
TACS	Total Access Communication Systems
TDD	Time Division Duplexing
TSR	Throughput Satisfaction Rate
TTI	Transmission Time Interval
UE	User Equipment
UL	Uplink
UMA	Unlicensed Mobile Access
UMTS	Universal Mobile Telecommunications System
UpPTS	Uplink Pilot Time Slot
VoIP	Voice over Internet Protocol
W-CDMA	Wideband Code Division Multiple Access
Wi-Fi	WLAN based on any IEEE 802.11 standards
WiMAX	Worldwide Interoperability of Microwave Access
WLAN	Wireless Local Area Network
WMN	Wireless Mesh Network
WPA	WiFi Protected Access
WSN	Wireless Sensor Network
xDSL	Digital Subscriber Line

ABSTRACT

Femto Access Points (FAPs) significantly improve indoor coverage and quality of service. FAPs are small, inexpensive, low-power base stations that are generally consumer deployed. However, due to high density of FAPs, many new challenges have not been sufficiently addressed such as resources allocation and interference mitigation. In resolving resource allocation problem, user mobility dynamics make it difficult to associate the best spectrum set of frequency/time resources with each FAP in order to deliver the users' data. The problem addressed is the determination of optimal resource allocation while user mobility dynamics are incorporated based on their position with time, while maintaining required quality of service (QoS). Prominent existing solutions which considered centralized, distributed and hybrid centralized/distributed scalable strategies are studied in literature. However, the impact of user mobility dynamics was not considered. To utilize spectrum resource more efficiently, a resource allocation mechanism that exploits the mobility of users in Orthogonal Frequency Division Multiple Access (OFDMA)-based femtocell networks known as Mobility-aware Femtocell Cluster-based Resource Allocation (M-FCRA) is presented. M-FCRA anchors upon an existing FCRA algorithm to ensure optimal resource allocation with mobility-awareness. M-FCRA has been validated by performing comparison and evaluation with FCRA algorithm. From the simulation results obtained using LTE-Sim simulator software, M-FCRA outperforms the existing state-of-the art FCRA approach in terms of Throughput Satisfaction Rate (TSR) and Spectrum Spatial Re-use (SSR). Moreover, the capacity and quality of service improvement in the network are of benefit to operators by offloading macrocell traffic hence low operating expenditures. Finally, users enjoy uninterrupted traffic indoors under mobility.

CHAPTER ONE

1.0 INTRODUCTION

1.1 BACKGROUND

Mobile broadband is growing fastest in developing countries, where 2013/2014 growth rates are twice as high as in developed countries [1]. According to the International Telecommunication Union (ITU), by end 2014, 44% of the world's households to have Internet access at home [1]. The higher percentage of indoor traffic is due to the increasing usage of applications on mobile devices such as Voice over Internet Protocol (VoIP), web browsing, video telephony, and video streaming, with constraints on delays and bandwidth requirements. This growing demand poses new challenges in the design of the future generation cellular networks. The ever increasing trend of indoor traffic contribution to overall mobile data traffic still degrades the user's quality of service (QoS). Indoor traffic offload from macrocell network to indoor network is necessary so as to maintain QoS.

Emergence of new devices and applications, and their usage pattern are responsible for growth of mobile data traffic. However, the high indoor penetration loss at higher Long-Term Evolution (LTE) frequencies decreases the overall capacity of the macrocell hence results in poor QoS for indoor users. This is a big challenge for operators to improve the capacity and quality of service of the network. The increasing growth requires increased network capacity which generates good revenue for operator's business model. Possible solutions that have emerged recently are deployment of femtocell and use of WiFi as presented in Section 2.4.

According to 3rd Generation Partnership Project (3GPP) specifications [2], LTE-based femtocell on Orthogonal Frequency Division Multiple Access (OFDMA), supports a wide range of multimedia and Internet services even in high mobility scenarios. Therefore, it has been designed to provide high data rates, low latency, and an improved spectral efficiency with respect to previous 3rd Generation (3G) networks. In this context, the design of effective resource allocation strategies becomes crucial. In fact, the efficient use of radio resources is essential to meet the system performance targets and to satisfy user needs according to specific QoS requirements [3].

In this thesis a mobility-aware resource allocation algorithm is developed and analysed in relation to impact of user mobility dynamics in femtocell network – indoor network in terms of throughput satisfaction rate and spectrum spatial reuse. In order to achieve this, split spectrum technique (macro and femtocells do not share spectrum) is assumed to manage interference between macro and femto network. From an operator's point of view, this thesis highlights the system reliability and quality of service which could be of interest for business model.

1.2 PROBLEM STATEMENT

It is essential to efficiently utilize radio resource to deliver services to mobile subscribers. Under a densely deployed femtocell, especially in indoor urban set up, resource allocation becomes a challenge in high users' mobility scenarios. Moreover, due to the impact of interference, some frequency/time resource blocks cannot be utilized simultaneously. This is also a challenge toward universal frequency reuse and frequency/time resource allocation in femtocell network. Therefore, it is difficult to associate the best spectrum set of frequency/time resources with each Femto Access Point (FAP) in order to deliver the users' data, while minimizing the gap between the required and allocated tiles at the same time minimizing interference between FAPs. The addressed problem is optimal resource allocation in femtocell network with users' mobility awareness based on their position with time, while maintaining required quality of service so as to enjoy uninterrupted data traffic. This work proceeds to study the impact of incorporating mobility dynamics in resource allocation algorithm.

1.3 JUSTIFICATION

The emergence of new technologies such as 4^{th} Generation (4G) due to need for higher data rates and mobile devices penetration has impacted on efficient use of radio resource. Consequently, need for data traffic offload to femtocell is eminent in indoor environment where macrocell coverage might be poor. Users' mobility dynamics in resource allocation therefore becomes fundamental in ensuring quality of service and femtocell network reliability. Several state-of-art resource allocation approaches have been proposed in literature. However, none of these approaches have considered users' mobility dynamics in resource allocation in a dense femtocell network. This research

work focused on incorporating user mobility dynamics such as changing position with time while maintaining the required QoS in the network. In OFDMA technology the number and positions of the femtocells are unknown, traditional network planning needs to be replaced by efficient spectrum allocation algorithms for the purpose of maintaining QoS, being novel algorithms still needed to perform such allocation in realistic scenarios. Therefore M-FCRA is presented in this work and results analysed.

1.4 OBJECTIVES

The objectives of this work are sub-divided into main and specific areas. The focus was to incorporate user mobility dynamics in resource allocation in femtocell network while maintaining the required QoS.

1.4.1 Main Objective

To develop a resource allocation algorithm based on min-max optimization for OFDMA femtocells network with users' mobility dynamics awareness.

1.4.2 Specific Objectives

(i) To formulate the mobility-aware resource allocation mathematically as a min-max optimization problem.

(ii) To simulate an efficient resource allocation algorithm based on min-max optimization to build disjoint femtocell clusters.

(iii) To analyse throughput satisfaction rate and spectrum spatial reuse as per the requirements of QoS under different Signal to Interference plus Noise Ratio (SINR).

(iv) To simulate M-FCRA allocation algorithm based on Min-Max Optimization for OFDMA Femtocell networks.

(v) To validate results of M-FCRA algorithm by comparing with the existing solutions of FCRA in terms of QoS metrics.

1.5 THESIS LAYOUT

The rest of the thesis is organized as follows: In Chapter 2, Cellular Network Technologies along with history of cellular network, global trends in data traffic, LTE overview and indoor solutions to data traffic are presented. Afterwards, resource

allocation approaches are provided in Chapter 3.The approach to resource allocation in LTE femtocell network under study is given in Chapter 4. This chapter includes mobility prediction model, M-FCRA resource allocation and optimization approach and detailed mathematical analysis. Simulation methodology and results along with their analysis are discussed in Chapter 5. In Chapter 6, conclusions are drawn from the results and future work proposed. Finally, published work arising from this research work are listed in Appendix A.

CHAPTER TWO

2.0 CELLULAR NETWORK TECHNOLOGIES

2.1 HISTORY OF CELLULAR NETWORKS

In early 1978, the United States of America (USA) started the Advanced Mobile Phone Systems (AMPS), widely known as 1st Generation (1G) analogue system. The performance of 1G system was limited by the poor performance of the analogue signal processing circuitry that struggled to combat the thermal noise generated by the system hardware [4]. The 1G analog mobile phones such as Total Access Communications Systems (TACS), Nordic Mobile Telephone (NMT), and AMPS among others [5]. In the early 1990s, the 2nd Generation (2G) system was introduced mainly in the USA, Europe and Japan, and was based on digital technology as in [4]. Subsequently, wireless communications have gained momentum and during the past two decades, experienced unforeseen growth worldwide mainly due to the invention of digital circuitry and devices, with much higher capacity than 1G systems as depicted in Figure 2.1 [6].

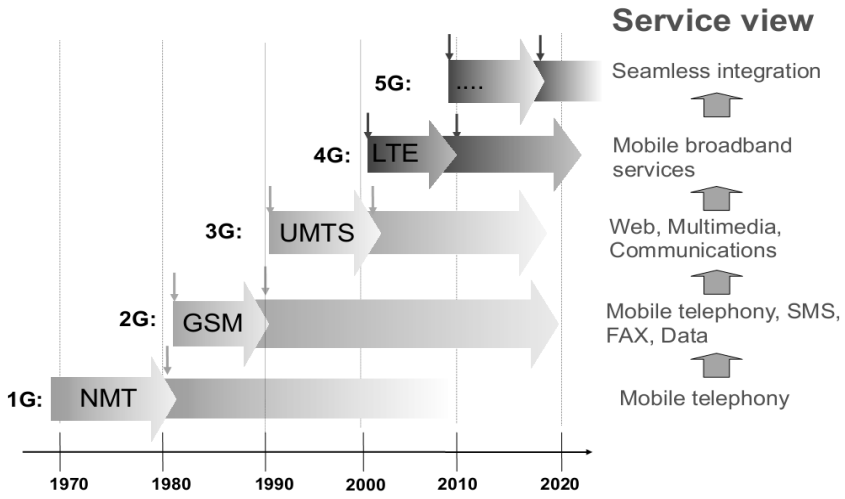

Figure 2.1 Cellular Network Evolution

They have also gradually become cheaper and more affordable for the wider population. Second generation (2G) included digital mobile phones such as global system for mobile communications (GSM), personal digital cellular (PDC), and digital

AMPS (D-AMPS) [7]. In [5], 3G systems were introduced across Europe predominantly as a mixed voice and data intensive service. With sophisticated digital signal processing, detection and estimation technology, 3G systems were capable of supporting several megabits per second data over a 10 MHz channel. This capacity enhancement triggered the introduction of multimedia services, digital audio and video streaming for mobile networks and devices. With the emergence of new high-end, hand-held devices and smart phones, users are tending evermore towards data intensive applications like network gaming, video conversation, online music, and video streaming, so the demand for high data rate services is increasing dramatically. This places tremendous pressure on network capacity and Quality of Service (QoS) requirement for mobile networks especially in indoor environment where macrocell coverage is poor. ITU recommendations for 4G systems envisages achieving a 1Giga bits per second (Gbps) data rate support for the downlink (DL) and 500Mbps for the uplink (UL) of stationary mobile stations (MS) [7].There is also a vision of achieving a DL data rate of 25 Gbps/km^2 [8]. The ABI Research predicts cellular-based Femtocells to outpace Unlicensed Mobile Access (UMA) and Session Initiation Protocol (SIP)-based Wi-Fi solutions by 2013 with application of next generation networks such as 4G LTE Advanced, that make use of OFDMA technology [9]. This research focused on development of resource allocation strategy with mobility dynamics awareness in OFDMA femtocell network based on min-max optimization problem.

2.2 GLOBAL TRENDS IN DATA TRAFFIC

Over the past few decades, the cellular communication industry has experienced a remarkable growth with the number of wireless subscribers reaching 7 billion by end 2014 [1]. Major part of these subscribers comprises of mobile users. Figure 2.2 shows the rate of increase of Mobile broadband users as compared with Fixed broadband [10] over the course of time. Mobile Broadband Bridges the Gap: Fixed Broadband and Mobile Subscriptions, 2009-2018 [11].

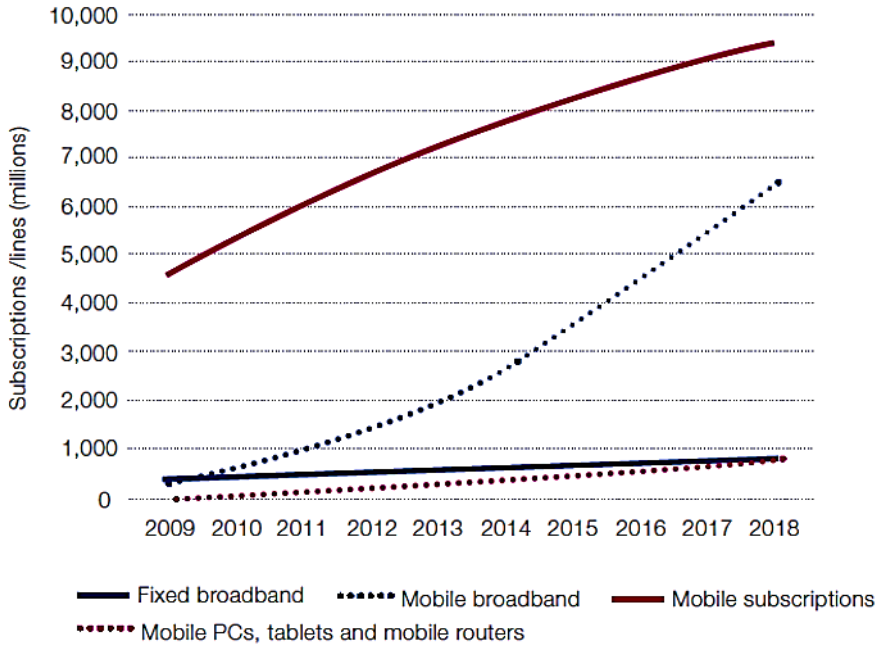

Figure 2.2 Fixed Broadband and Mobile Subscriptions, 2009-2018

Mobile devices and connections are not only getting smarter in their computing capabilities but are also evolving from lower-generation network connectivity (2G) to higher-generation network connectivity (3G, 3.5G, and 4G or LTE) as shown in Figure 2.3 [12]. When device capabilities are combined with faster, higher bandwidth and more intelligent networks, it leads to wide adoption of advanced multimedia applications that contribute to increased mobile and Wi-Fi traffic.

The explosion of mobile applications and phenomenal adoption of mobile connectivity by end users, on one hand, and the need for optimized bandwidth management and network monetization, on the other hand, is fuelling the growth of global 4G deployments and adoption.

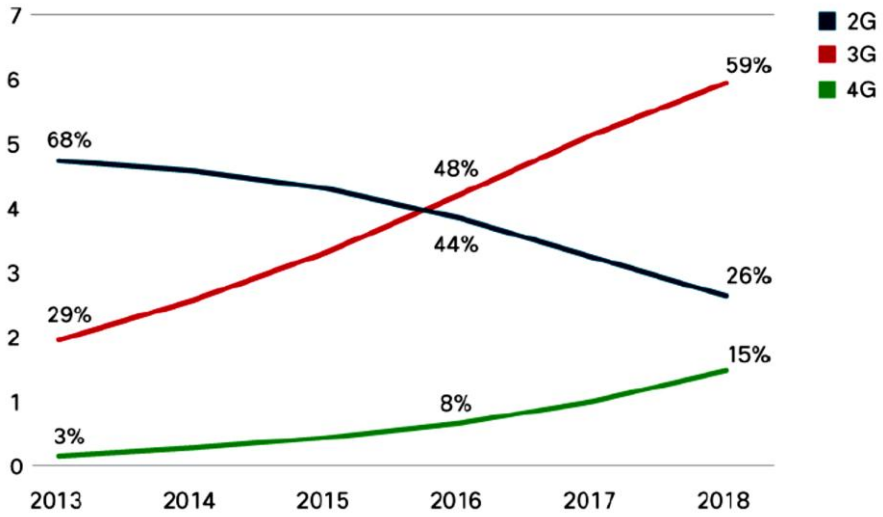

Figure 2.3 Global Mobile Devices and Connections by 2G, 3G, and 4G

It is interesting to note that the increase in the overall network traffic is due to packet data and not the voice traffic. Figure 2.4 highlights the rate of increase in the packet data over the wireless network [13]. Hence it makes it essential to analyse how the cellular networks are going to be affected by this boost in data traffic and what measures are needed to be taken to cope with such increasing demand [10].

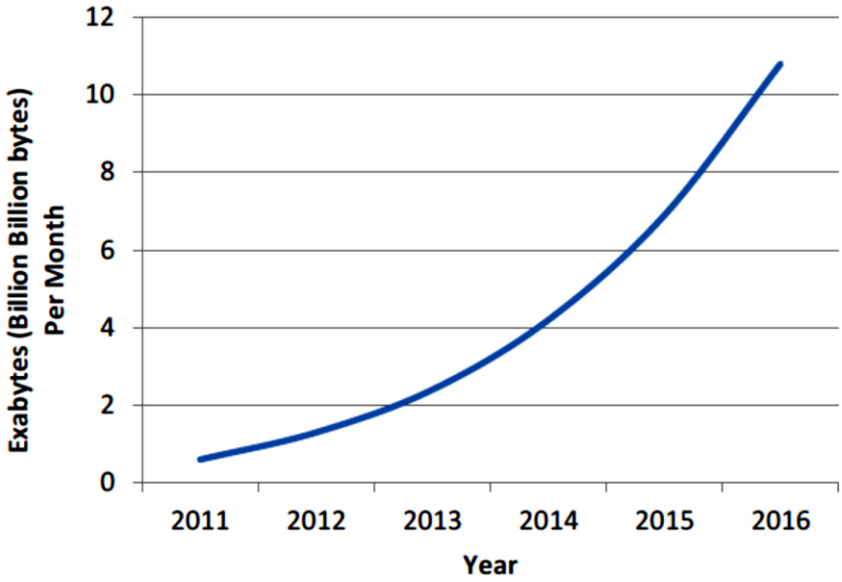

Figure 2.4 Global Mobile Data Growth

Higher frequency signals are more prone to the path loss and it widely affects the coverage area of a network cell as demonstrated in equation 2.1.

$$Free\ Space\ Path\ Loss\ (FSPL) = \left(\frac{4\pi d}{\lambda}\right)^2 \quad (2.1)$$

Where:

d is the distance of the receiver from the transmitter (metres)

λ is the signal wavelength (metres)

According to [14], as the number of indoor users increase, path loss shifts towards higher values in a Wideband Code Division Multiple Access (W-CDMA) network. Since LTE use higher frequency than Universal Mobile Telecommunications System (UMTS) and 3G networks, it is of core importance to analyse the effect of indoors users on higher frequency networks. The capacity of a network, according to Shannon's capacity theorem [15], is related to the amount of bandwidth available and is governed by the following equation.

$$C = B\log_2(1 + SINR) \quad (2.2)$$

As the number of femtocells deployed indoors increases, spectrum utilization and traffic offload analysis become important in this context. This makes findings of this work interesting as the number of indoor users as well as the demanded data rates to support emerging applications increase. Indeed provision of QoS to users in femtocell networks must be a priority of any network operator in this scenario. The next section provides an overview of the LTE networks as a solution to spectrum utilization and users' satisfaction.

2.3 OVERVIEW ON LTE NETWORKS

A deep understanding of radio propagation issues in cellular networks has driven the LTE standardization process towards the use of advanced and high performance techniques [16].

In fact, in order to efficiently support the current high variety of applications, LTE networks have been conceived with very ambitious requirements that strongly overtake features of 3G networks, mainly designed for classic voice services [2].

LTE aims, as minimum requirement, at doubling the spectral efficiency of previous generation systems and at increasing the network coverage in terms of bitrate for cell-

edge users [17]. Moreover, several new performance targets, with respect to other technologies, have been addressed during the standardization phase, spanning from increased data rates (i.e., the allowed peak data rates for the downlink and uplink are equal to 100 Mbps and 50 Mbps, respectively) to the support of very high user mobility. To make LTE networks highly flexible for a worldwide market, a variable bandwidth feature, that gives to network operators the possibility to throttle the bandwidth occupation between 1.4 and 20 MHz, is also included. Among all these performance targets, summarized in Table 2.1, the most important novelty introduced by LTE specifications is the enhanced QoS support by means of new sophisticated Radio Resource Management (RRM) techniques [17].

Table 2-1 Main LTE Parameters Targets

Parameter	**Target**
Peak Data Rate	- Downlink: 100 Mbps - Uplink: 50 Mbps
Spectral Efficiency	2 – 4 times better than 3G systems
Cell-Edge Bit-Rate	Increased whilst maintaining same site locations as deployed today
User Plane Latency	Below 5 ms for 5 MHz bandwidth or higher
Mobility	- Optimized for low mobility up to 15 km/h - High performance for speed up to 120 km/h - Maintaining connection up to 350 km/h
Scalable Bandwidth	From 1.4 to 20 MHz
RRM	- Enhanced support for end-to-end QoS - Efficient transmission and operation of higher layer protocols
Service Support	- Efficient support of several services (e.g, web-browsing, video-streaming, VoIP) - VoIP should be supported with at least a good quality as voice traffic over the UMTS network

LTE has been designed as a highly flexible radio access technology in order to support several system bandwidth configurations (from 1.4 MHz up to 20 MHz). Radio spectrum access is based on the Orthogonal Frequency Division Multiplexing (OFDM) scheme. In particular, Single Carrier Frequency Division Multiple Access (SC-FDMA) and OFDMA are used in uplink and downlink directions, respectively. Differently from basic OFDM, they allow multiple access by assigning sets of sub-carriers to each individual user. OFDMA can exploit sub-carriers distributed inside the entire spectrum, whereas SC-FDMA can use only adjacent sub-carriers. OFDMA is able to provide high scalability, simple equalization, and high robustness against the time-frequency selective nature of radio channel fading. On the other hand, SC-FDMA is used in the LTE uplink to increase the power efficiency of UEs, given that they are battery supplied [17].

Radio resources are allocated into the time/frequency domain [18] as shown in Figure 2.5. In particular, in the time domain they are distributed every Transmission Time Interval (TTI), each one lasting 1 ms, the time is split in frames, each one composed of 10 consecutive TTIs. Furthermore, each TTI is made of two time slots with length 0.5 ms, corresponding to 7 OFDM symbols in the default configuration with short cyclic prefix. In the frequency domain, instead, the total bandwidth is divided in sub-channels of 180 kHz, each one with 12 consecutive and equally spaced OFDM sub-carriers. A time/frequency radio resource spanning over two time slots in the time domain and over one sub-channel in the frequency domain is called Resource Block (RB) and corresponds to the smallest radio resource unit that can be assigned to an UE for data transmission. As the sub-channel size is fixed, the number of RBs varies according to the system bandwidth configuration (e.g., 25 and 50 RBs for system bandwidths of 5 and 10 MHz, respectively). N_{FB}^{DL} is the symbol used to indicate the maximum number of downlink Resource Blocks for a given bandwidth.

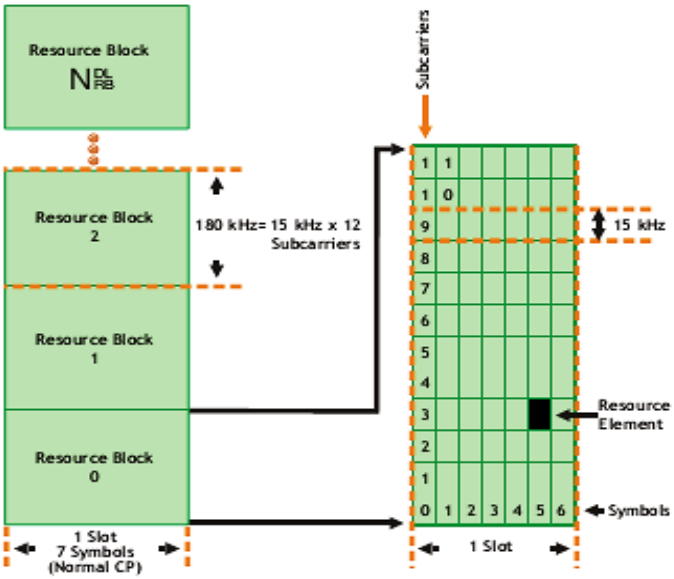

Figure 2.5 Relationship between a slot, symbols and Resource Blocks

As described in [18], the LTE radio interface supports two types of frame structure, related to the different duplexing schemes. Under Frequency Division Duplex (FDD), the bandwidth is divided in two parts, allowing simultaneous downlink and uplink data transmissions, and the LTE frame is composed of 10 consecutive identical sub-frames.

2.3.1 LTE Frame Structures

According to [19], T_s is the basic time unit for LTE. Time domain fields are typically defined in terms of T_s. T_s is defined as $T_s = 1/(15000 \times 2048)$ seconds or about 32.6 nanoseconds.

Downlink and uplink transmissions are organized into frames of duration $T_f = 307200\ T_s$.

The 10 ms frames divide into 10 subframes. Each subframe divides into 2 slots of 0.5 ms. In the time domain, a slot is exactly one Resource Block long. Two frame types are defined for LTE: Type 1, used in Frequency Division Duplexing (FDD) and Type 2, used in Time Division Duplexing (TDD).

Type 1 frames consist of 20 slots with slot duration of 0.5 ms as shown in Figure 2.6. Type 2 frames contain two half frames as shown in Figure 2.7. Depending on the switch period, at least one of the half frames contains a special subframe carrying three fields of switch information: Downlink Pilot Time Slot (DwPTS), Guard Period (GP)

and Uplink Pilot Time Slot (UpPTS). If the switch time is 10 ms, the switch information occurs only in subframe one. If the switch time is 5 ms, the switch information occurs in both half frames, first in subframe one, and again in subframe six. Subframes 0 and 5 and DwPTS are always reserved for downlink transmission. UpPTS and the subframe immediately following UpPTS are reserved for uplink transmission. Other subframes can be uplink or downlink. Timing and symbol allocations shown for FDD with normal cyclic prefix (CP). Special fields are shown in subframes 1 and 6. Guard period separates the Downlink and Uplink. This TDD example represents a 5 ms switch point. A 10 ms switch point would not have the special fields in subframe 6. The relationship between bandwidth and resource block is explained next.

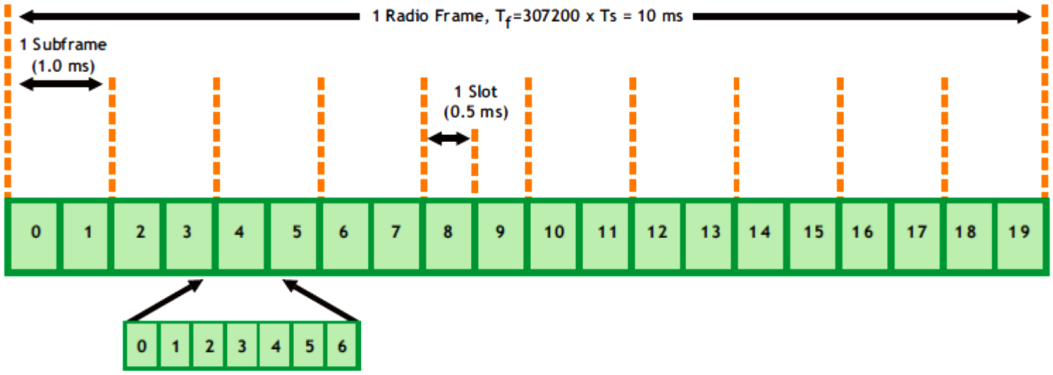

Figure 2.6 Type 1 Frame

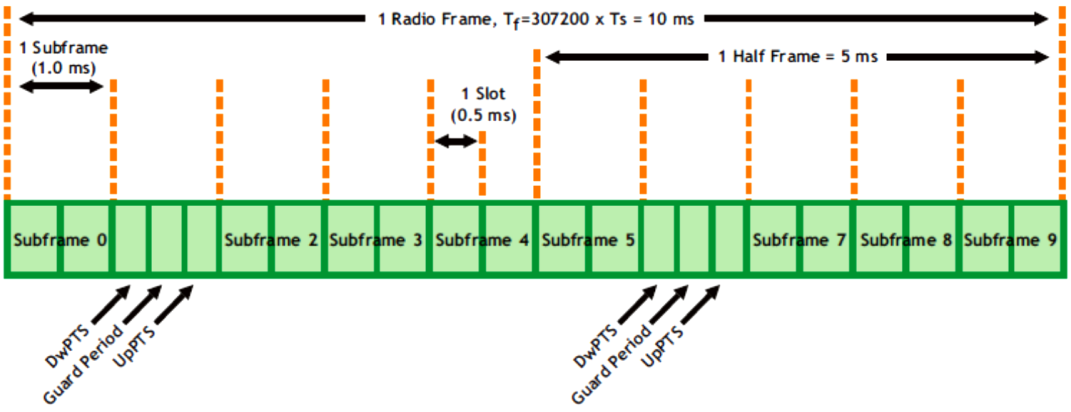

Figure 2.7 Type 2 Frame

2.3.2 Relationship between Bandwidth and Resource Block

LTE Physical layer deals with parameters like frequency, bandwidth, Modulation, cyclic prefix, coding rate which play importance in calculation of the throughput as described in [20]. LTE system uses OFDMA as access technology in downlink to increase the spectral efficiency and SC-FDMA in uplink due to low Peak to Average Power ratio (PAPR) advantage. LTE supports both TDD and FDD duplexing, flexible bandwidth i.e.1.4, 3, 5,10,15,20 MHz and modulation schemes QPSK, 16 QAM, 64 QAM.

As discussed in section 2.3.1, in LTE, ten 1 ms subframes compose a 10 ms frame. Each subframe divides into two slots. The smallest modulation structure in LTE is the Resource Element. A Resource Element is one 15 kHz subcarrier by one symbol. Resource Elements aggregate into Resource Blocks. A Resource Block has dimensions of subcarriers by symbols. Twelve consecutive subcarriers in the frequency domain and six or seven symbols in the time domain form each Resource Block.

The number of symbols depends on the Cyclic Prefix (CP) in use. When a normal CP is used, the Resource Block contains seven symbols. When an extended CP is used, the Resource Block contains six symbols. A delay spread that exceeds the normal CP length indicates the use of extended CP.

As shown in Figure 2.8, Channel Bandwidth is the width of the channel as measured from the lowest channel edge to the highest channel edge. The channel edge is the centre frequency ± (channel bandwidth/2). Transmission Bandwidth is the number of active Resource Blocks in a transmission. As the bandwidth increases, the number of Resource Blocks increases. The Transmission Bandwidth Configuration is the maximum number of Resource Blocks for the particular Channel Bandwidth as shown in Table 2.2. The maximum occupied bandwidth is the number of Resource Blocks multiplied by 180 kHz [19].

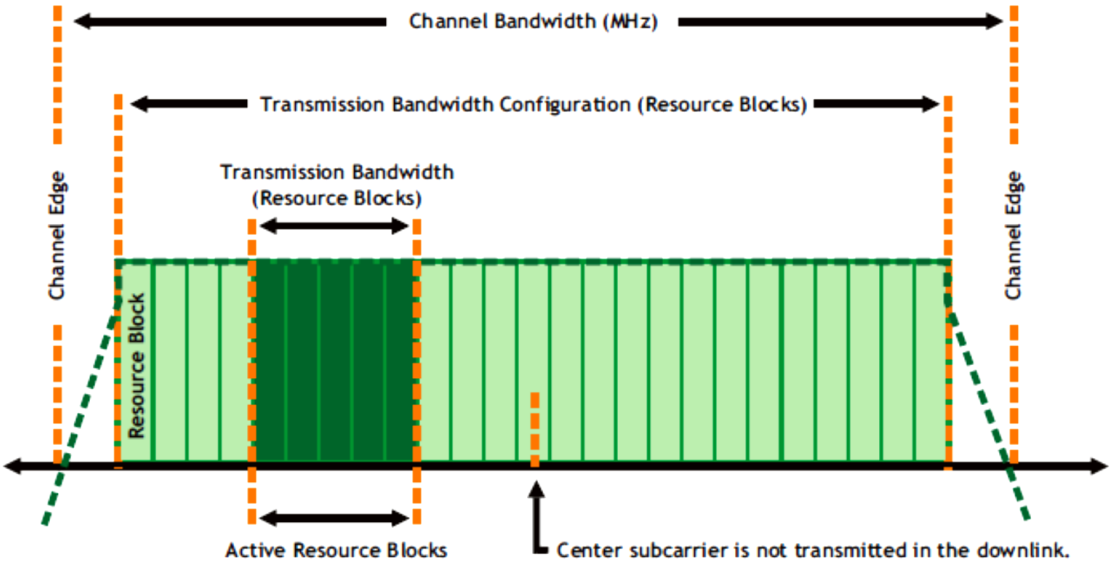

Figure 2.8 Resource Block, Channel and Transmission Bandwidth

Bandwidth directly affects the throughput. Different BWs have different number of RBs.

Table 2-2 Transmission Bandwidth Configuration

Channel Bandwidth (MHz)	Maximum Number of Resource Blocks (Transmission Bandwidth Configuration)	Maximum Occupied Bandwidth (MHz)
1.4	6	1.08
3	15	2.7
5	25	4.5
10	50	9.0
15	75	13.5
20	100	18.0

Calculation to find the numbers of subcarriers and Resource Blocks is presented in [20]. 10% of total bandwidth is assumed to be used for guard band. Though 10% guard band assumption is not valid for 1.4 MHz bandwidth. Taking 20MHz as an example, 10% of 20 MHz is 2 MHz, used as guard band, thus effective bandwidth will be 18MHz. Number of subcarriers = 18 MHz/15KHz = 1200 and Number of Resource Blocks =18 MHz/180KHz = 100.

2.3.3 Throughput Calculation in LTE Systems

As presented in the previous section, for any system throughput is calculated as symbols per second. Further it is converted into bits per second depending on the how many bits a symbol can carry.

In LTE for 20 MHz, there are 100 Resource Blocks and each Resource block has 12x7x2=168 Symbols per ms in case of Normal CP.

So there are 16800 Symbols per ms or 16800000 Symbols per second or16.8 Msps. If modulation used is 64 QAM (6 bits per symbol) then throughput will be 16.8x6=100.8Mbps for a single chain.

For a LTE system with 4x4 MIMO, Four Transmission Four Receiver (4T4R), the throughput will be four times of single chain throughput. i.e. 403.2 Mbps. Many simulations and studies show that there is 25% of overhead used for Controlling and signalling. So the effective throughput will be 300 Mbps.

The 300 Mbps number is for downlink and not valid for uplink. In uplink there is only one transmit chain at UE end. So with 20 MHz a maximum of 100.8Mbps as calculation shown above is achieved. After considering 25% of overhead we get 75Mbps in uplink.

This is the number of throughput 300Mbps for Downlink and 75Mbps for Uplink shown everywhere is arrived at [20].

2.3.4 WCDMA compatibility issues with LTE

The main LTE parameter targets were presented in section 2.3.3. Currently 3G system is using Wideband Code Division Multiple Access (WCDMA) access technique with a bandwidth of 5 MHz both in uplink and downlink. In WCDMA different users are assigned different Walsh codes [21]which are multiplexed using same carrier frequency. In downlink, transmission is orthogonal, due to fixed eNodeB with no multipath, hence the Walsh codes received are synchronized at UEs. While in case of multipath, Walsh codes received are not orthogonal anymore and hence results in Inter Symbol Interference (ISI). The ISI can be eliminated with advanced receiver such as Linear Minimum Mean Square Error (LMMSE) receiver.

In order to achieve high data rates, the interference problem increases in WCDMA when used with LTE due to multipath for larger bandwidths such as 10 MHz or 20

MHz. This is because of high chip rates in higher bandwidths, which is small in case of lower bandwidths. Similarly complexity of LMMSE also increases due to increased multipath in large bandwidths. It is also possible to add multiple carriers of 5 MHz to support large bandwidth. However, it increases the complexity of eNodeB and UE. Another issue with WCDMA is that a bandwidth less than 5 MHz will not be supported by LTE, as LTE supports smaller bandwidths as well. WCDMA only supports multiples of 5 MHz [21].

After careful consideration of LTE flexibility, scalability and compatibility issues associated with WCDMA, it was necessary to employ a new access technique for LTE system. The following section presents an alternative technique for LTE system.

2.3.5 OFDMA

OFDMA approach was first proposed by R.W Chang [21], [22] a few decades ago and analysed later by Slatzberg [21], [23]. In OFDMA the whole bandwidth is divided into small subcarriers or parallel channels which is then used for transmission with reduced signalling rate.

These subcarriers are orthogonal which means that they do not correlate with each other. The subcarrier frequency is shown in the equation given below:

$$f_k = k\Delta f \tag{2.2}$$

where Δf is the subcarrier spacing. Subcarrier is first modulated with a data symbol of either 1 or 0, the resulting OFDMA symbol is then formed by simply adding the modulated carrier signal. This OFDM symbol has larger magnitude than individual subcarrier and thus having high peak value which is the characteristics of OFDMA technique.

LTE takes advantage of OFDMA, a multi-carrier scheme that allocates radio resources to multiple users. OFDMA uses Orthogonal Frequency Division Multiplexing (OFDM) [19]. For LTE, OFDM splits the carrier frequency bandwidth into many small subcarriers spaced at 15 kHz, and then modulates each individual subcarrier using the QPSK, 16-QAM, or 64-QAM digital modulation formats. OFDMA assigns each user the bandwidth needed for their transmission. Unassigned subcarriers are off, thus reducing power consumption and interference.

OFDMA uses OFDM; however, it is the scheduling and assignment of resources that makes OFDMA distinctive. The OFDM diagram in Figure 2.9 below shows that the entire bandwidth belongs to a single user for a period. In the OFDMA diagram, multiple users are sharing the bandwidth at each point in time. Each color represents a burst of user data. In a given period, OFDMA allows users to share the available bandwidth.

Figure 2.9 OFDM vs. OFDMA.

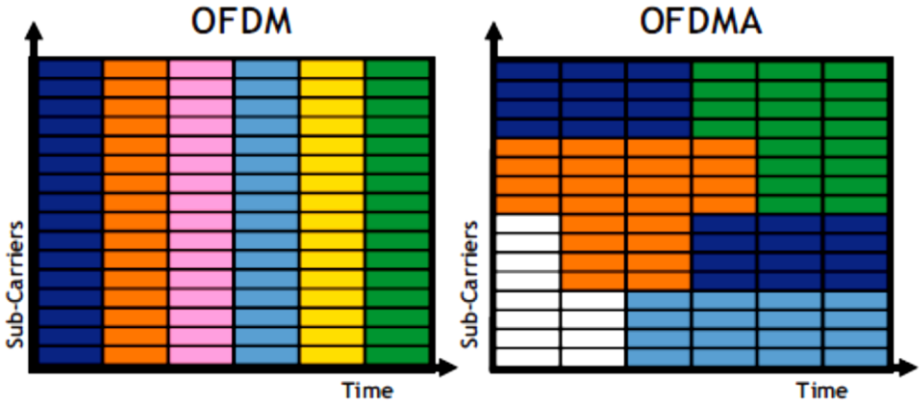

2.3.6 SC-FDMA

In the uplink, LTE uses a pre-coded version of OFDM called SC-FDMA. SC-FDMA

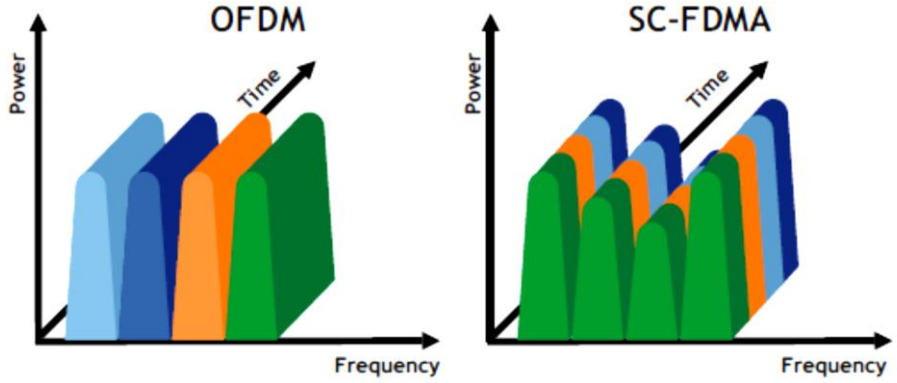

Figure 2.10 Frequency Component of OFDM vs SC-FDMA

has a lower PAPR (Peak-to-Average Power Ratio) than OFDM. This lower PAPR reduces battery power consumption, requires a simpler amplifier design and improves uplink coverage and cell-edge performance. As shown in Figure 2.10, in SC-FDMA,

data spreads across multiple subcarriers, unlike OFDMA where each subcarrier transports unique data. The need for a complex receiver makes SC-FDMA unacceptable for the downlink [19]. In OFDM, each frequency component carries unique information. In SC-FDMA, the information is spread across multiple subcarriers.

2.3.7 Adaptive Modulation and Coding (AMC)

Adaptive Modulation and Coding refers to the ability of the network to determine the modulation type and the coding rate dynamically based on the current RF channel conditions reported by the UE in Measurement Reports [19]. The RF digital modulation used to transport the information is QPSK, 16-QAM, and 64-QAM. Figure 2.11 below shows the ideal constellations for each modulation where each dot represents a possible symbol. In the QPSK case, there are four possible symbol states and each symbol carries two bits of information. In 16-QAM, there are 16 symbol states. Each 16-QAM symbol carries 4 bits. In 64-QAM, there are 64 symbol states. Each 64-QAM symbol carries 6 bits. Higher-order modulation is more sensitive to poor channel conditions than the lower-order modulation because the detector in the receiver must resolve smaller differences as the constellations become more dense.

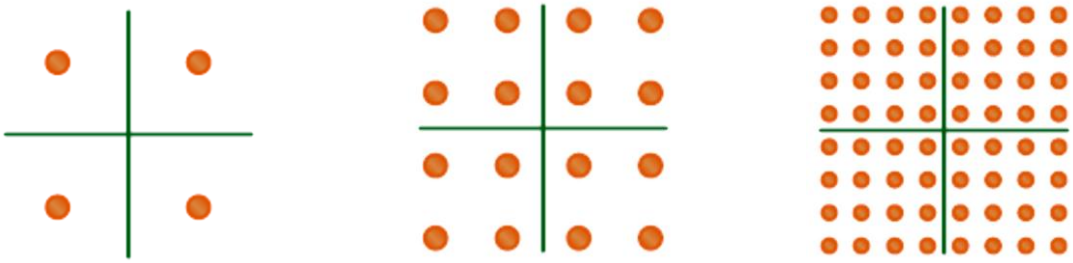

QPSK (4-QAM) 2 bits per symbol 16-QAM 4 bits per symbol 64-QAM 6 bits per symbol

Figure 2.11 Modulation order

Coding refers to an error-correction methodology that adds extra bits to the data stream that allow error correction. Specified as fractions, Code Rates specify the number of data bits in the numerator and the total number of bits in the denominator. Thus if the Code Rate is 1/3, protection bits are added so one bit of data is sent as three bits [19].

2.4 INDOOR SOLUTIONS

As mentioned in Chapter 1, increase in the overall cellular traffic is mainly due to indoor users. In order to cope with this ever increasing demand of bandwidth, there is a dire need to come up with a solution. WiFi and femtocells, both present an attractive alternative. The pros and cons of each of them are separately highlighted in the next two sections.

2.4.1 WiFi

WiFi refers to wireless communication standard IEEE 802.11 [24]. The most recent standard is IEEE 802.11n [19] which can provide peak data rate up to 75 Mbps. As there is high penetration of WiFi access points and WiFi enabled devices, WiFi can be an attractive solution for indoor traffic-offload for mobile operators.

WiFi works in an unlicensed spectrum but has no independent voice service and could result in higher latencies for the voice packets. Also, the WiFi protocol does not ensure the secure communication due to the vulnerability of its protocols such as WiFi Protected Access (WPA) [24].

2.4.2 Femtocell

Femtocells are small, inexpensive, low-power base stations that are generally consumer-deployed and connected to their own wired backhaul connection [25]. In this respect, they resemble WiFi access points, but instead they utilize one or more commercial cellular standards and licensed spectrum. Femtocell uses a low power Femto Access Point (FAP) that utilizes fixed broadband connections to route femtocell traffic to cellular networks. Moreover, it is a part of self-organizing network (SON) with zero touch installation. It supports limited number of active connections 3 or 4 but can be extended from 8 to 32. It is used to improve indoor signal strength as it avoids walls penetration loss [26].

Femtocells can support indoor users with high signal strength and thus can offload these users from outdoor base stations. The main driver for the user is improved coverage and capacity thus offers better quality of service, not only to indoor users but also to outdoor users by offloading traffic.

Femtocell uses the licensed spectrum owned by a mobile operator. Smaller cells are typically used in homes and there is an option for enterprise femtocells. As femtocell can connect user's mobile phone with home network, it can be seen as true initiative for fixed mobile convergence [26].

2.4.3 Choice of indoor solution

For the scope of this research work, we chose femtoells as the indoor solution to offload the indoor traffic due to several of the above reasons. It is also critical to highlight the commercial aspect of deployment of femtocells and how, for operators, it would affect the management of the network.

Femtos provide quick solution to meet high capacity requirements wherever needed. Capital

(CapEx) and Operational (OpEx) Expenses are much lower as compared to deployment of a macro site. They are also compatible with high frequency Next Generation Technologies (e.g.

LTE).

CHAPTER THREE

3.0 RESOURCE ALLOCATION APPROACHES

3.1 POWER AND SUB-CARRIER ALLOCATION IN OFDMA DOWNLINK

The work of Wong et al. in [27], is among the first and most cited papers which investigates the problem of dynamic resource allocation in the downlink of multiuser OFDM systems. They formulate an optimization problem, assuming perfect knowledge of the instantaneous channel gains for all users, to minimize the total transmit power subject to given transmission rate requirements. They show that this optimization problem is a combinatorial optimization problem and in order to make it tractable, they relax the integer constraint. Then, they prove that the new problem is a convex minimization problem, for which they derive the necessary iterative algorithm for calculating the Lagrangian multipliers. Since their optimal solution is based on the relaxation method, they introduce a sub-optimal multi-user adaptive OFDM (MAO) scheme and show that its performance is not far from the optimal continuous one. Despite the significant gain over fixed assignment schemes, their algorithm is difficult to implement and requires a large number of iterations to converge.

In [28], Rhee et al. formulate another optimization problem that maximizes the Shannon capacity for the worst user, based on the total power constraint in the downlink of a multi-user OFDM system. They also relax the integer constraint (allow for subchannel sharing among user) and convert the problem into a convex optimization problem. Then, they propose a sub-optimal algorithm with a low complexity to allocate the subchannels to users. It is shown that their sub-optimal algorithm performs almost as good as the optimal solution with a 2%–4% gap. Later, Kim et al., in [29], convert the above originally non-linear optimal resource allocation problems, into linear ones and solve them by integer programming (IP). To reduce the complexity, they proposed a sub-optimal approach, which allocates the subcarriers based on the Linear Programming (LP) relaxation of the IP. Then, they use a greedy algorithm for bit loading. Their results show that the sub-optimal method produces almost the same results as the optimal one, with significant lower complexity.

Based on the optimization problem in [27], Kivanc et al., in [30], derive a computationally inexpensive method for subcarrier and power allocation in the downlink. Again, the objective is to minimize the total power consumption subject to a given minimum transmission rate requirement for each user. The allocation algorithm is divided into two steps. In the first step, the bandwidth assignment based on Signal to Noise Ratio (SNR) (BABS) greedy algorithm uses the average SNR values to calculate the number of subcarriers that each user will get. In the next step, the specific assignment of subcarriers is done, for which they provide two different greedy algorithms. The first algorithm, Rate Craving Greedy (RCG), allocates each subcarrier to the user with the maximum transmission rate on that subcarrier. In the second algorithm, Amplitude Craving Greedy (ACG), the subcarrier is given to the user which has the highest gain on that subcarrier, given that the user has not exceeded the number of subcarriers calculated from the first step. Their proposed algorithms have comparable performance to the iterative one in [27], while being computationally cheap. More different approaches for dynamic resource allocation in OFDMA downlink can be found in [31], [32], [33], [34] [35].

3.2 POWER AND SUB-CARRIER ALLOCATION IN OFDMA UPLINK

Regarding the OFDMA uplink subcarrier and power allocation, in [36], Kim et al. formulate a sum-rate optimization problem based on the Shannon capacity formula for the Gaussian channel. The difference in their optimization problem with the usual downlink problems is that they consider each user has a specific power constraint in the uplink. Moreover, the allocated power of one user to a subcarrier can differ from the allocated power of another user to the same subcarrier. Therefore, in their proposed optimization approach, power plays an important role. To solve the optimization problem, they relax the integer constraint on the assignment variable and prove that for the solution to be optimal, the assignment variable should have binary values. Therefore, the relaxation does not violate the intrinsic feature of OFDMA. Then, they propose a greedy algorithm for subcarrier allocation and an iterative water-filling power allocation algorithm. In the subcarrier allocation algorithm, first, the assigned power for all subcarrier/user pairs are calculated, either by using the water-filling algorithm or equal power distribution. Afterwards, each subcarrier is assigned to the

user with the largest marginal rate. It is shown that their sub-optimal algorithms outperform the downlink algorithms. Their results also showed that the equal power distribution and water-filling algorithm in the uplink have similar performances. In [37], Shen et al. investigate the design trade-offs in the OFDMA uplink with respect to subcarrier assignment methods in different applications. They show that, for fixed and portable applications, where the propagation channels are almost static, the maximum throughput can be achieved when subcarriers are assigned to users with minimum frequency diversity, and for mobile services, the assignment method with maximum frequency diversity provides the maximum throughput.

All of the above dynamic resource allocation schemes, in the uplink (as well as the downlink) of OFDMA systems, assume a perfectly synchronized system (transmitter and receiver) and they do not take the multiple access interference (MAI) into account. MAI refers to the interference between direct-sequence users. This interference is the result of the random time offsets between signals, which make it impossible to design the code waveforms to be completely orthogonal. While the MAI caused by any one user is generally small, as the number of interferers or their power increases, MAI becomes substantial [38].

3.3 LOAD BALANCING

In cellular networks, coordinated scheduling of UEs over a set of cells helps to improve load balancing throughout the cellular network [39], [40], [41]. Basically, the main aim was to select one cell at a time by considering congestion level or channel quality measurement over multi-cell environment (categorized into a cell breathing approach), contributing to load balancing [42]. Researchers [43] characterize radio resource allocation for 3G networks with an empirical study, and demonstrate that traffic patterns critically affect radio resource and energy consumption but fails to incorporate user mobility scenarios which is the main focus of this work.

Resource management schemes in femtocell networks [44], [45] are recently investigated. In wireless Local Area Networks (LAN), load balancing approaches based on a cell breathing technique [46] or by checking the overload level [47], [48] are taken for improving throughput and mitigating cell delay. To achieve efficient resource allocation for mobile users in wireless Access Points (AP) networks, the

authors [49] propose a dynamic association scheme by predicting the next reliable AP cell that a mobile user will likely connect to and hand-overing to it. Recently, researchers have considered more on volatile wireless link due to relatively low power wireless vagary and mobility in the cell selection and resource allocation problem for wireless networks.

For load balancing in heterogeneous networks, efficient radio interface selection schemes between 3G and Wi-Fi, and among 802.11, Bluetooth, and ZigBee are studied in [50], [51] [52], [53]. Also, the authors [54], [55] focus on the radio resource management problem in 3G and WLAN for smooth transition between interfaces with QoS. However, the two crucial domains of efficient radio interface selection and resource management have not been tightly coupled, and accordingly need to be more explored although some researchers [56], recently started proposing a game-theoretical cell selection and resource allocation for LTE and WiMAX networks. Also, the cell selection and resource allocation problem explicitly considering overload scenarios and mobility dynamics have not been relatively well studied.

3.4 DISTRIBUTED RESOURCE ALLOCATION IN AD-HOC NETWORK

Several dynamic clustering strategies have been proposed in [57], [58], [59], [60]. The strategies differ in the criteria used to organize the clusters and in the implementation of the distributed clustering algorithms. However, none of them uses prediction of node mobility as a criterion for cluster organization.

The (α, t)-Cluster framework, in [61] defines a strategy for dynamically organizing the topology of an ad-hoc network in order to adaptively balance the trade-off between pro-active and demand-based routing by clustering nodes according to node mobility is presented. However, this framework does not focus on the topology of a Wireless Mesh Network (WMN).

A clustering algorithm for "quasistatic" ad hoc networks, where nodes are static or moving at a very low speed was proposed in [62]. The proposed scheme is more adapted to the Wireless Mesh Networks (WMN) environment. However, it is concerned with one-hop clustering, which defeats the purpose of clustering in WMNs. This approach focused on mobility of nodes but not users in resource allocation.

In [63], a new heuristic for electing multiple leaders in ad hoc networks called Max-Min Leader Election in Ad Hoc Networks is presented. However, the clusters have the same radius, an additional constraint, which may lead to unsatisfactory results regarding the Radio Resource Utilization (RRU) cost minimization.

In [64], the authors demonstrate how certain geometric properties of the wireless networks can be exploited to perform clustering with some desired properties. Generic graph algorithms developed for arbitrary graphs would not exploit the rich geometric information present in specific cases such as the wireless network environment.

The authors in [65] used Connected Dominating Set (CDS), clustering approach in mobile ad hoc networks, based on graph theory. In this approach, the objective is to identify the smallest set of Cluster Heads (CHs) that forms a CDS. The set of CHs operates therefore as routers and forms a virtual backbone for the ad hoc network. However, the proposed scheme is concerned with one-hop clustering, which defeat the purpose of WMNs.

In [66], clustering algorithms in the context of Wireless Sensor Networks (WSNs) are presented. The common criterion for the selection of CHs with these algorithms is based on the energy consumption constraint. Instead, efficiently using the wireless resources is the main concern in WMNs and is crucial to achieve acceptable performance.

In [67], a clustering algorithm to integrate the WMNs with the wired backbone is presented. The authors investigated the well-known problem of gateway placement in WMNs. In this study, the focus is on each macro-cluster instead of virtual clustering.

In [68], authors investigated the radio resource utilization efficiency in WMNs. They propose two clustering schemes to improve the resource utilization in such networks. Based on both analytical models and simulations, they proved that clustering is not helpful for slow mobile users with high data traffic loads. They showed that the Distributed Clustering Algorithm (DCAM) stands out as the best solution for both small-to-moderate and highly connected wireless mesh networks, whereas the Optimal Static Clustering (OSC) scheme is the best solution for both large and low-connected networks. Finally, they showed that the DCAM clustering technique handles better the changes in the physical topology due to Access Point (AP) failures or addition. Typically, the OSC clustering scheme needs several hours up to days to reconfigure

the network according to the new optimal disjoint-cluster placement as opposed to the instantaneous DCAM reconfiguration.

Clustering in ad-hoc networks mostly focus on efficient handling of the frequent network topological changes due to ad-hoc nodes mobility. The main objective has therefore been to adapt quickly to topological changes, which occurs only occasionally in femtocell networks, due to their relatively static topologies as described in [69].

The distributed resource allocation algorithm namely Distributed Random Access (DRA), which is more appropriate for medium-wide networks, is described in [44]. The resources, represented as time-frequency slots (tiles) are orthogonalized between macrocells and femtocells based on the gradient ascent/descent heuristic. However, due to its pseudo-random nature, QoS cannot be guaranteed by such an approach and the throughput satisfaction rate of femtocells has not been considered in the analysis.

A fully distributed and scalable algorithm for interference management in LTE-Advanced environments has been presented in [70]. The proposal called Autonomous Component Carrier Selection (ACCS) is executed locally in each femtocell. However, the scheme is highly correlated with the environmental sensing since it mainly relies on measurement reports. In addition, ACCS does not allocate time-frequency slots but only subcarriers, which can be expensive and penalizing in terms of bandwidth.

A decentralized F-ALOHA spectrum allocation strategy for two-tier cellular networks is described in [71]. The proposal is based on a partition of the spectrum between the macrocell and femtocells. However, F-ALOHA cannot guarantee any level of QoS since it is based on a pseudo-random algorithm. In addition, this scheme does not consider time-frequency slots as resources and instead, it focuses on sub-carriers allocation.

3.5 CENTRALISED RESOURCE ALLOCATION IN FEMTOCELL NETWORK

Three resource allocation algorithms in OFDMA femtocells are proposed in [72]. The first method is called orthogonal assignment algorithm. It divides the spectrum into two independent sets S_M and S_F used by the macrocells and femtocells, respectively. The problem is to find the best split that maximizes the satisfaction of the required QoS. However, this scheme does not take into account the femto-to-femto interference, which remains an important issue for indoor performance, especially

when femtocells are densely deployed. The second method is called co-channel assignment algorithm *FRSx*. Here macrocells can use the entire spectrum, but each femtocell uses only one random fragment. The interference between femtocells is indeed reduced by a factor of *x*. However, no details are given to find its optimal value. The last method is called Centralized-Dynamic Frequency Planning (C-DFP). In this method, femtocells send their request to a centralized node in the backhaul to find the best resource allocation for each femtocell. This scheme can easily converge to the optimum. However, it is practicable only for small-sized femtocell networks.

Resource management in OFDMA-based femtocell networks is an ongoing research area. In [69], FCRA a new scalable resource allocation strategy based on clustering is proposed. A distributed clustering algorithm to form disjoint femtocell clusters is described. The objective is to subdivide the resource allocation problem into sub-problems by means of clustering and the use of optimum centralized spectrum allocation inside each cluster to handle more efficiently the available resources. However, the authors did not incorporate the impact of user mobility dynamics to their study, instead assumed that users were static.

In this research work, M-FCRA algorithm based on Min-Max Optimization analyses the impact of incorporating user mobility dynamics in frequency/time allocation algorithm in femto cellular networks. Specifically, this work focuses on incorporating user mobility dynamics in resource allocation algorithm and study its impact by considering the variation in their positions with time. A detailed presentation of FCRA is provided in the following sub-section.

3.6 FEMTOCELL CLUSTER-BASED RESOURCE ALLOCATION SCHEME (FCRA)

3.6.1 System description

As stated in the previous section, FCRA is a hybrid distributed/centralised spectrum allocation approach. FCRA considered a macrocell embedded with a set *F* of Femtocell Access Points (FAPs) that represent residential or enterprise networks.

The study focussed on the downlink communications. FCRA was then to find the optimal allocation of resources dedicated for femtocells to deliver the users data, while

minimizing the interference between femtocells and at the same time ensuring the required QoS.

For each femtocell $F_a \in F$, a set of interfering femtocells, denoted by I_a was defined. This set depends on the minimum required Signal to Interference plus Noise Ratio (SINR) values and the indoor path loss model. As in [70], the latter is modelled based on A1-type generalized path loss models for the frequency range 2-6 GHz developed in WINNER [73]. In addition, for each femtocell F_a the binary resource allocation matrix denoted by Δ_a, with 1 or 0 in position (i, j) according to whether the tile (i, j) is used or not.

To represent the users' demands, a vector V_a whose elements correspond to the bandwidth required by users associated with the femtocell F_a was introduced as shown in equation 3.1.

$$V_a = \begin{bmatrix} v_1 \\ v_2 \\ \vdots \\ v_i \end{bmatrix} \tag{3.1}$$

where $v_{1,} v_2 \ldots v_i$ are required tiles (time-frequency slots) by user i. The total number of tiles required by femtocell F_a to fulfill the attached users' demands denoted by:

$$R_a = \sum_{i=1}^{n_a} V_a\,(i) \tag{3.2}$$

where n_a is the total number of users belonging to femtocell F_a. Total number of required tiles (tiles are the radio resource represented as time-frequency slots) R_a is not constant and depends on the arrival/departure process of end users.

3.6.2 WINNER II Path Loss Model

The Wireless World Initiative New Radio (WINNER) which developed the WINNER II path loss model is a consortium of partners with the goal of enhancing mobile communication performance. The WINNER II path loss is also semi empirical and allows for a flexible modelling of propagation channels in a wide range of scenarios including indoor offices, indoor-outdoor and urban micro-cell. The indoor path loss P_l incorporated in this research is the WINNER II A1 line of site (LOS) and non-LOS (NLOS), as specified in [73] and given below;

$$P_{l(LOS)} = 46.8 + 18.7\, log_{10}(d) + 20\, log_{10}\left(\frac{f_c}{5}\right) \quad (3.3)$$

$$P_{l(NLOS)} = 46.4 + 20\, log_{10}(d) + 20\, log_{10}\left(\frac{f_c}{5}\right) + L_w \quad (3.4)$$

Where;

f_c is carrier Frequency

d is the distance in meters between FAP and UE

L_w is the wall penetration losses which is $5(n_w - 1)$ for light walls

$n_w$is the number of walls

3.6.3 Assumptions

1. Both FAPs and the macrocell are to operate using the same OFDMA technology. Similar to [6], an OFDMA frame structure that is populated with time-frequency slots, so-called tiles was considered.
2. Resources are split between the macrocell and femtocells, thus eliminating interference between femto/macro users. This kind of spectrum partition aims at maximizing the throughput and fairness within the macrocell and femtocells as presented in, [44] [72].
3. R_a is updated periodically every epoch δ_t.
4. The number of end users that can be associated with each femtocell follows a random uniform distribution with a maximum value of 4 per femto.
5. Femtocells adopt the Round Robin strategy to serve the associated users, [44] [70].

3.6.4 Problem formulation

The objective of FCRA was to find the optimal resource allocation of a set of tiles in each femtocell to deliver the users data, while minimizing the interference between femto cells and at the same time ensuring the required QoS as earlier mentioned in section 2.3. To do so, a new metric, called throughput satisfaction rate per femtocell, which is defined as the ratio of the received number of allocated tiles to the total

requested ones for each femtocell was introduced. The aim was then to maximize this metric. Objective function will be to minimize the maximum gap between the number of allocated and required tiles in each FAP (i.e., the worst case is optimized). Given the set of interferer femtocells I_a, $\forall F_a \in F$ and for every epoch δ_t, the Min-Max optimization problem was formulated as illustrated below:

$$min\left[max_a\left(\frac{R_a - \sum_{i,j}\Delta_a(i,j)}{|F| \times R_a}\right)\right] \qquad \forall F_a \in F \qquad (3.5)$$

Subject to:

(a) $\forall F_a \in F$: $\sum_{i,j}\Delta_a(i,j) \leq R_a$

(b) $\forall i,j, \forall F_a \in F\ , \forall F_b \in I_a$: $\Delta_a(i,j) + \Delta_b(i,j) \leq 1$

(c) $\forall i,j, \forall F_a \in F$: $\Delta_a(i,j) \in \{0,1\}$

The objective function, (equation 3.5), is to minimize the maximum difference between the required and allocated tiles. Condition (a) denotes that the resource scheduler must guarantee that femtocells cannot obtain more than the required spectrum, and inequality (b) ensures that two interfering femtocells cannot use the same tiles. The resource allocation problem has been proved to be NP-hard (NP stands for Non-deterministic Polynomial time) [74]. Clustering approach was used to subdivide the problem into subproblems [69]. In the next subsection a detailed description of FCRA scheme is presented.

3.6.5 FCRA Algorithm

In this section, a hybrid FCRA algorithm for OFDMA femtocell networks is presented. This approach is based on three main components:

(i) Cluster formation,

(ii) Cluster-head resource allocation and

(iii) Resource contention resolution.

First, FCRA builds disjoint clusters within the network. Then, a cluster-head resolves resource allocation problem and allocates resources to all femtocells within. A cluster head is femtocell with the highest interference degree among its one-hop neighbours. Each cluster may interfere with its neighbours because the cluster-head resolution does not consider the neighbour clusters' allocation. Hence, a resource contention

avoidance is also considered to resolve collision in subsequent frames. The three stages are detailed as follows [69].

(i) Cluster formation stage

First, each femtocell created its one-hop neighbour list containing the identity of its interfering femtocells (i.e., causing interference to its users). This was reached by sensing the environment exploiting users' measurement reports. The list was then transmitted and shared with the corresponding one-hop neighbours. Every FAP computed the number of interfering femtocells (i.e., interference degree) of each of its one-hop neighbours. A cluster-Head (CH) was elected based on this information as the one deciding on the resource allocation. It was then notified to the other Cluster-Members (CMs). Each FAP determined whether it can act as CH or CM. Indeed, a femtocell was elected as CH if it had the highest interference degree among its one-hop neighbours. In this case, all associated one-hop neighbours acted as CMs and were attached to the elected CH. Otherwise, the femtocell was considered as CM and attached to the elected CH among its immediate neighbours (if it exists). If more than one unique CH was chosen, the one with the highest interference degree was considered as CH in order to minimize the tiles' collision between femtocells (if equal degrees, a random tie-break is used). However, if no CH is chosen by the neighbourhood's femtocells (i.e., all neighbours act as CMs and are associated to other clusters), the FAP was attached to the cluster of the neighbour with the highest interference degree. The FCRA Algorithm flowchart is presented in Figure 3.1.

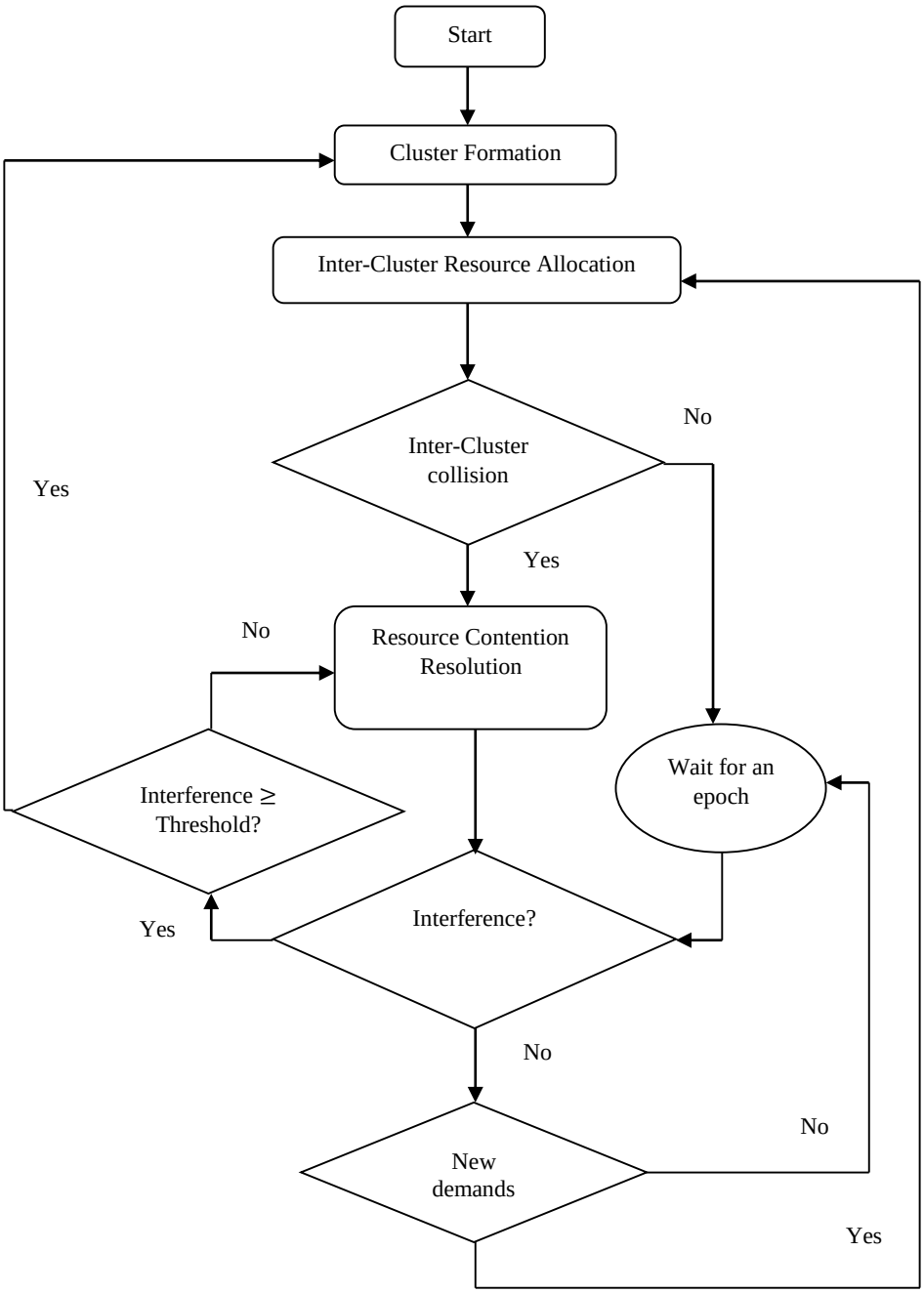

Figure 3.1 FCRA Algorithm Flowchart

(ii) Cluster-head resource allocation stage

Once the femtocell network is partitioned in clusters, the CH jointly allocated resources to all femtocells within each cluster. The objective was to satisfy as much as possible the femtocells' requirement in terms of tiles while avoiding interference within the cluster. To achieve this, each CH resolves individually the above resource

allocation problem every epoch δ_t. It is worth noting that, since the obtained clusters' size was not large, the CH resolution using a solver such as ILOG CPLEX [75], converged within a short period T_{conv}. This allowed femtocells to serve their attached users in a timely manner. However, it was noted that users at the edge of two neighbouring clusters might still interfere when they operate on the same resources. This could indeed happen since each CH resolves the above mentioned problem independently from its neighbouring clusters. Consequently, two interfering femtocells attached to different clusters could use the same allocated tile. To resolve such collision, a simple coordination mechanism was realized and detailed in the next subsection.

(iii) Resource contention resolution stage

As mentioned earlier, two femtocells associated with different CHs, but interfering with each other, might have been assigned the same tiles from their respective CHs. Thus, interference occurs between their associated end users. In this case, each user suffering from contention sends a feedback report to its associated femtocell to notify about the collision on the selected tile. Then, each femtocell samples a Bernoulli distribution to resolve contention on the collided tiles. Accordingly, it decided whether the attached user would keep using the tile or would remove it from the allocated resources. If collision occurs, FCRA converges to a stationary allocation within a small number of frames. Hence, the solution is practically feasible [69].

3.6.6 Performance metric

The performance of FCRA was evaluated based on the output of the optimization problem resolution for each constructed cluster. QoS metrics considered were Throughput Satisfaction Rate (TSR) and Spectrum Spatial Reuse (SSR).

(i) Throughput Satisfaction Rate

According to [69], throughput satisfactory rate is the average degree of satisfaction of a femtocell with respect to the requested resources. For each femtocell F_a, $TSR(F_a)$ was defined as the ratio of the received number of allocated tiles to the total requested ones, expressed as follows:

$$TSR(F_a) = \left(\frac{\sum_{i,j} \Delta_a(i,j)}{R_a}\right) \tag{3.6}$$

Where;

F_a is a femtocell in the set F of femtocells

R_a is the total number of tiles required by femtocell F_a

$\Delta_a(i,j)$ is the binary resource allocation matrix, with 1 or 0 in position (i,j) according to whether the tile (i,j) is used or not.

The TSR metric thus given by:

$$TSR = \sum_{F_a \in F} \left(\frac{TSR(F_a)}{|F|}\right) \tag{3.7}$$

(ii) Spectrum Spatial Reuse (SSR)

Spectrum Spatial Reuse is the average portion of femtocells using the same elementary resource block (tile) within the network. Therefore, it is defined as the mean value of tiles' spatial reuse. The SSR metric is thus expressed as follows:

$$SSR = \frac{1}{M \times |F|} \sum_{i,j} \sum_{F_a \in F} \Delta_a(i,j) \tag{3.8}$$

Where;

M is equal to the length of OFDMA frame (downlink) in terms of tiles (time-frequency slots)

F_a is a femtocell in the set F of femtocells

F is a set of femtocells

$\Delta_a(i,j)$ is the binary resource allocation matrix, with 1 or 0 in position (i,j) according to whether the tile (i,j) is used or not.

3.6.7 Performance evaluation of FCRA

Both centralized optimal (C-DFP [72]) and distributed resource allocation (DRA [44]) schemes were used as benchmarks to which the FCRA potential benefits were compared. The gain of FCRA studied when the users are static using several arbitrary FAPs topologies and under various interference level scenarios. Results obtained using the solver "ILOG CPLEX" [75] were reported. A total of 31 simulations were run and mean value calculated with confidence level fixed to 99.70%. In each simulation, the number of mobile nodes attached to each femtocell and their traffic demands were varied.

The analysis was achieved using a typical OFDMA frame (downlink LTE frame) consisting of M= 100 tiles (time-frequency slots), as in [6]. Users were distributed uniformly within the femtocells with a maximum value of 4 per FAP. Each user uniformly generated its traffic demand (required bandwidth), which was translated into a certain number of tiles V_a ($0 \leq V_a \geq 25$). The F femtocells were distributed randomly in a 2-D 400 M $\times$ 400 M area, with one FAP randomly placed in each 10 M $\times$10 M residence. Then, based on the SINR values and the path loss model [73], of WINNER II channel models as in section 3.5.1 (b), the interference matrix I_a for every femtocell F_a was derived. In the simulations, different SINR thresholds: 10, 15, 20 and 25 *dB* were considered to show the impact of the interference degree on the evaluated metrics. FCRA algorithm used a Bernoulli distribution to resolve the resource contention problem. Hence in the experiments, set mean of Bernoulli was 0.5. Consequently, femtocells have the same chance to use or discard the collided tile.

3.6.8 Suggested approach

The problem addressed is the determination of optimal resource allocation while user mobility dynamics are incorporated based on their position with time, while maintaining required quality of service (QoS).

Prominent existing solutions which considered centralized, distributed and hybrid centralized/distributed scalable strategies are studied in literature. However, impact of user mobility dynamics was not considered in the study of resource allocation.

To utilize spectrum resource more efficiently, a resource allocation mechanism that exploits the mobility of users in Orthogonal Frequency Division Multiple Access (OFDMA)-based femtocell networks known as Mobility-aware Femtocell Cluster-based Resource Allocation (M-FCRA) is presented. M-FCRA anchors upon an existing FCRA algorithm to ensure optimal resource allocation with mobility-awareness.

CHAPTER FOUR

4.0 PROPOSED MOBILTY-AWARE ALGORITHM: M-FCRA

4.1 INTRODUCTION

The most considered approaches include centralized, distributed and hybrid centralized/distributed scalable strategies [69]. However, the authors did not incorporate user mobility dynamics in their studies. Based on the review of related work on mobility-aware resource allocation approaches, an efficient method is therefore presented that consists of formulation of the resource allocation mathematically as a min-max optimization problem and an appropriate hybrid centralized/distributed algorithm involving three main phases is developed:

(i) Cluster formation
(ii) Cluster-head resource allocation with user mobility awareness
(iii) Resource contention resolution.

As mentioned earlier, FCRA considered static users in the network, while, M-FCRA incorporates the mobility trace of mobile users in resource allocation and studied its impact. This study focused on the second stage and the rest are explained as follows:

4.1.1 Cluster formation

When powered on, a FAP will listen to surrounding transmissions (i.e., neighbouring FAPs' control channel and reference signal transmissions) and gather information through measurements collected from users attached to it or via a receiver function within the FAP also called Sniffer [76]. Based on this information, each FAP computes the number of interfering femtocells and transmit it along with its Physical Cell Identity (PCI) to each one of them. This information exchange was done using over-the-air via UE approach according to 3GPP [76] . For DL, a victim UE forwards interference coordination related information to the aggressor femtocell. Therefore each FAP had a list containing the interference degree of neighbouring femtocells and decided whether it was a CH, or was attached to a neighbouring cluster. The CH election algorithm is described as follows:

- Each femtocell elects the CH as the one with the highest interference degree among its one-hop neighbours;
- If it is not CH itself, the femtocell acts as a Cluster-Member (CM) of a CH chosen by its immediate neighbours;
- If more than one unique CH is chosen by the neighbouring femtocells, the one with the highest interference degree is elected as CH in order to minimize the collision of tiles between femtocells (if equal degrees, a random tie-break is used);
- If no CH is chosen by the neighbouring femtocells (i.e., all neighbours act as CMs and are already associated to other clusters), the femtocell is attached to the cluster of the neighbour with the highest interference degree. It is worth noting that to avoid large cluster size due to the attachment of such femtocells to neighbouring clusters, we set a threshold on its size denoted by CS_{th}. When the threshold is reached, the corresponding femtocell will act as an isolated CH.

It was noted that time synchronization between femtocells is necessary to enable accurate resource allocation decisions. The most and simple used one is timing from the Internet. Indeed, once turned on, and before initiating any communication, femtocells get synchronized to the cellular core network using an asymmetric communication link, such as DSL technologies, thanks to an enhanced version of IEEE 1588 [77].

4.1.2 Cluster-head resource allocation with user mobility awareness

Once the femtocell network was partitioned into clusters, the second step was to jointly allocate resources to all FAPs within each cluster taking into account QoS requirements of attached mobile users. To achieve this, each cluster-member reported to its corresponding CH the required resources to satisfy its attached and predicted mobile user's demands.

The solution of the resource allocation problem was attained by resolving sequentially the two objectives of the problem with user mobility considered since the obtained

clusters' size was not large with FAP activity factor of 0.5. The activity factor is the ratio of active to inactive cells at any given time. CH resolved the problem using "IBM ILOG CPLEX" [75] solver.

4.1.3 Resource contention resolution.

According to the previous stage, users at the edge of two neighbouring clusters might still interfere when they operate on the same resources. This could indeed happen since each CH resolves the resource allocation problem independently from its neighbouring clusters. Consequently, two interfering femtocells attached to different clusters could use the same allocated tile. To resolve such collisions, a simple yet efficient mechanism can be realized and described as follows:

- Each user suffering from contention sent a feedback report (as of 3GPP specifications [76]) to its associated femtocell to notify it about the collision on the selected tile;
- Each femtocell tried to resolve contention on the collided tiles by sampling a Bernoulli distribution. Accordingly, it decided whether the attached user would keep using the tile or would remove it from the allocated resources.

If collision occurred, M-FCRA converged to a stationary allocation within a short time period, hence the solution became practically feasible.

4.2 NETWORK MODEL

In this section, first, system network and mobility models used are defined. Then, resource allocation as a multi-objective min-max optimization problem is formulated.

The network considers an OFDMA femtocell network (e.g., LTE) consisting of several FAPs representing residential or enterprise networks, as shown in Figure 4.1 [78].

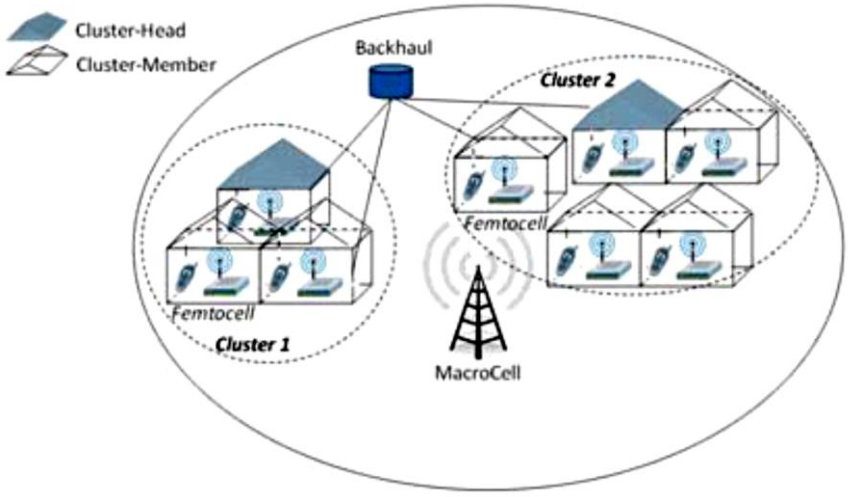

Figure 4.1 Network model

As in [79], [80] [81], M-FCRA adopts an orthogonal channel assignment that eliminates the cross-layer interference between femtocells and the macrocell. This study focussed on the downlink communications based on OFDMA, whose frame structure can be viewed as time-frequency resource blocks, also called tiles.

As previously mentioned in section 2.3, a tile is the smallest unit of resource that can be assigned to a user and corresponds to 0.5 ms and 180 KHz frequency band. According to the LTE specification [82], scheduling is done on a subframe basis for both the downlink and uplink. Each subframe consists of two equally sized slots of 0.5 ms in length. A certain number of users attach to each FAP; user demands represent the required bandwidth, expressed in number of required tiles. The relation between required tiles of user i (D_i) and the throughput requirement (TP_i^{req}) can be written as follows [83]:

$$D_i = \left\lceil \frac{TP_i^{req}}{\psi . eff_i} \right\rceil \tag{4.1}$$

Where;

$\psi = (SC_{ofdm} \cdot SY_{ofdm})/T_{subframe}$ is a fixed parameter that depends on the network configuration

SC_{ofdm} is the numbers of subcarriers

SY_{ofdm} is the number of symbols per tile

$T_{subframe}$ is the frame duration in time domain

In LTE specification [82], SC_{ofdm} = 12, SY_{ofdm} = 7, and $T_{subframe}$ = 0.5 ms. The parameter eff_i is the efficiency (bits/symbol) of the used Modulation and Coding Scheme (MCS).

The aim of this work is to incorporate and study the impact of user mobility in resource allocation in femtocell network. Users have open access to any femtocell. Only data communication is considered ignoring symbols used for scheduling information, as well as a fixed transmission power for all FAPs [44], [71], [72] [84], [85].

In urban dense environment, it is expected that often the sum of demands of the FAPs exceeds the available resources. Therefore, the objective for this research is to find, for such congestion situations, an efficient resource allocation strategy that takes care of throughput expectations while controlling the interference between femtocells and at the same time taking into account the QoS requirements of users is necessary. Since the total amount of network resources is limited, an optimal resource allocation strategy in femtocell network is then needed. Any user is indeed allocated the required bandwidth (tiles) only when the network has sufficient resources to meet the QoS requirements.

4.3 MOBILITY PREDICTION MODEL

Mobility prediction guarantees continuous service delivery to mobile users, and efficient resource allocation in femtocell network. Mobile operators try to know the next mobile's location using mobility prediction. It consists of locating in advance the next connection point in order to anticipate resource allocation at the predicted point [86].

The mobility prediction model considered is based on Markov chains, exploiting the mobility trace of the mobile user, in the context of LTE architecture in [87], [88]. It

exploits a sequence of femtocells that mobile users cross during an interval of time as depicted in Figure 4.2. This model has been proved to be efficient enough to predict the movements changes of a mobile user [86]. The model is based on two complementary prediction algorithms, the Global Prediction Algorithm (GPA), and the Local Prediction Algorithm (LPA). Both algorithms use the mobility trace of the users as follows:

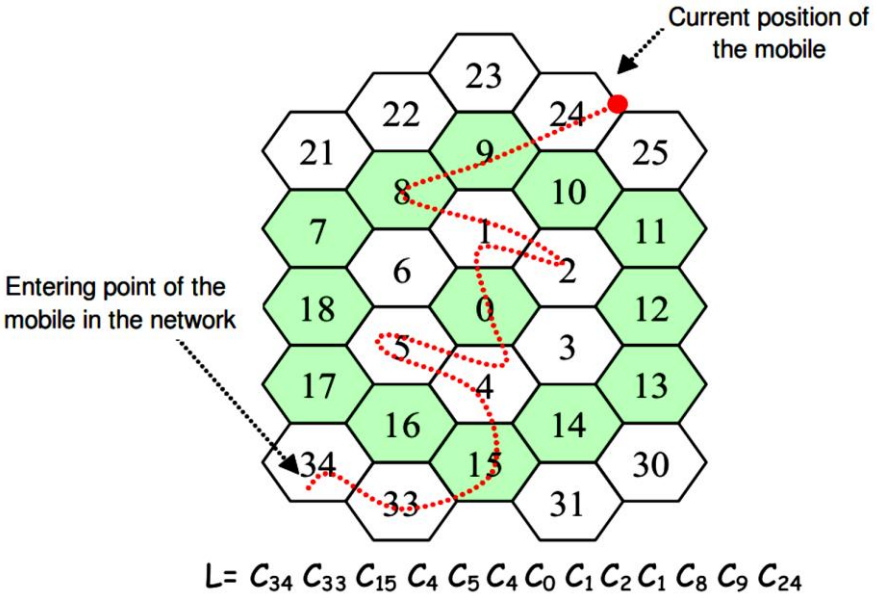

Figure 4.2 Example of mobility trace

4.3.1 Global Prediction Algorithm

GPA allows prediction of regular movements of a mobile client. It is based on the user's mobility trace and a second order continuous-time Markov chain, whose discrete states are the femtocells of the network. Thus, the transition probability to the next femtocell to be visited by a mobile user depends not only on its current femtocell but also on the previously visited femtocell. The mobility trace consists of the identity of all femtocells crossed by the mobile user, during a fixed time period.

For each mobile user, the GPA computes the transition probabilities from its current femtocell F_z to each femtocell in its neighbourhood (adjacent femtocells) noting I_b. A tuple (M, N, r) is defined for each femtocell F_z where:

- For each pair of femtocells F_c and F_d in I_b, $M(F_d, F_z, F_c)$ is the number of transitions of the mobile user from femtocell F_z to femtocell F_c in the past, knowing that each time such a transition occurred the mobile user was previously in femtocell F_d.
- $N(F_d, F_z)$ is the number of transitions of the mobile user from femtocell F_d to femtocell F_z.
- $r(F_z)$ indicates the average residence time of a mobile user in femtocell F_z.

Assumptions

$V = F_1F_2F_3 \ldots F_{f-1}F_f$ be the mobility history trace of a mobile user.

$X = F_{f-1}F_f$ be the sequence, in V, of the previously visited femtocell and the current femtocell of the mobile user. $Y = F_fF_{f+1}$ is the sequence of the current femtocell and the future femtocell to be visited, the estimated transition probability P_e is given by:

$$P_e = P\left(\frac{X_{f+1} = Y}{X_f = X}\right) = \frac{M(X, F_{f+1})}{N(F_{f-1}, F_f)} \tag{4.2}$$

4.3.2 Local Prediction Algorithm

If the GPA is unsuccessful, LPA uses a first order continuous-time Markov chain. The transition probability from the current femtocell F_f to each adjacent femtocell $F_{f+1}$is given by:

$$P_m = P\left(\frac{X_{f+1} = Y}{X_f = X}\right) = \frac{N(F_f, F_{f+1})}{Z(F_f)} \tag{4.3}$$

Where;

$Z(F_f)$ is the number of times femtocell F_f appears in the mobility trace.

The prediction based on first order Markov chain may fail if the current cell F_f appears for the first time in the trace. In this case, the visits frequency $H(F_f)$ from adjacent femtocells is used. If B is the total number of adjacent femtocells to F_f,

$$H(F_F) = \sum_{f=1}^{B} Z(F_f) \tag{4.4}$$

So, the transition probability to an adjacent femtocell is given by:

$$P_m = \frac{Z(F_f)}{H(F_f)} \tag{4.5}$$

To complete mobility prediction model, at every entered femtocell F_f, the algorithm computes the transition probability to every adjacent femtocell of F_f. The algorithm checks if there are enough information in the mobility trace to predict the next femtocell:

- If enough information is gathered, the GPA is used and P_e is computed (Equation 4.2)
- Otherwise, the LPA is used and P_m is computed using Equation 4.3 or Equation 4.5, according to the value of $N(F_f, F_{f+1})$.

This prediction procedure just needs to know the adjacent femtocells. This information was provided by analysing the received SINR signals.

In order to overcome the real-time constraint faced by resource allocation problem, incorporation of mobility dynamics is presented. Knowing the next visited femtocell provides more time to mobile users to negotiate with cluster-head to generate synchronized resource allocation that maximizes throughput. When a mobile user enters a new femtocell, a new stage t in its mobility begins. Every mobile user has a unique identifier id which is characterised by requested bandwidth (tiles) at every

stage t. The CH compares all predicted probability of connections and assigns the femtocell with highest probability of 1. The resource requested is assumed guaranteed and every prediction is successful thus; $P = 1$, otherwise 0, where $P \in \{P_e, P_m\}$. At every stage t, the mobile user id is attached to a femtocell. Its terminal executes the mobility prediction algorithm in order to compute the transition probability from the current femtocell to every adjacent femtocell in the list I_b. The mobile terminal then communicates this prediction results to the attached FAP. With the help of its FAP, mobile user id initiates the resource allocation reservation with the predicted femtocell through CH. At stage $t + 1$, mobile user id enters a new femtocell with its requested resource reallocated by new FAP.

4.4 MIN-MAX OPTIMIZATION PROBLEM

The min-max optimization algorithm was designed for simultaneous minimization and maximization of the same objective function. The aim of the optimization problem is to maximize the overall utilization of resource blocks with QoS constraints. The idea is to minimise the maximum gap between the number of allocated and capacity tiles (frequency/time) feasible for each FAP while incorporating mobility dynamics.

The flowchart in Figure 4.3 represents an existing algorithm with a modification of additional constraint [69]. User mobility constraint is added in an existing approach to create a mobility aware scheme for resource allocation in OFDMA femtocells network. The network has been configured to recognize user mobility dynamics while finding the optimal resource allocation of a set of tiles (frequency/time blocks) in each

FAP to deliver the users data, at the same time ensuring the required QoS is maintained.

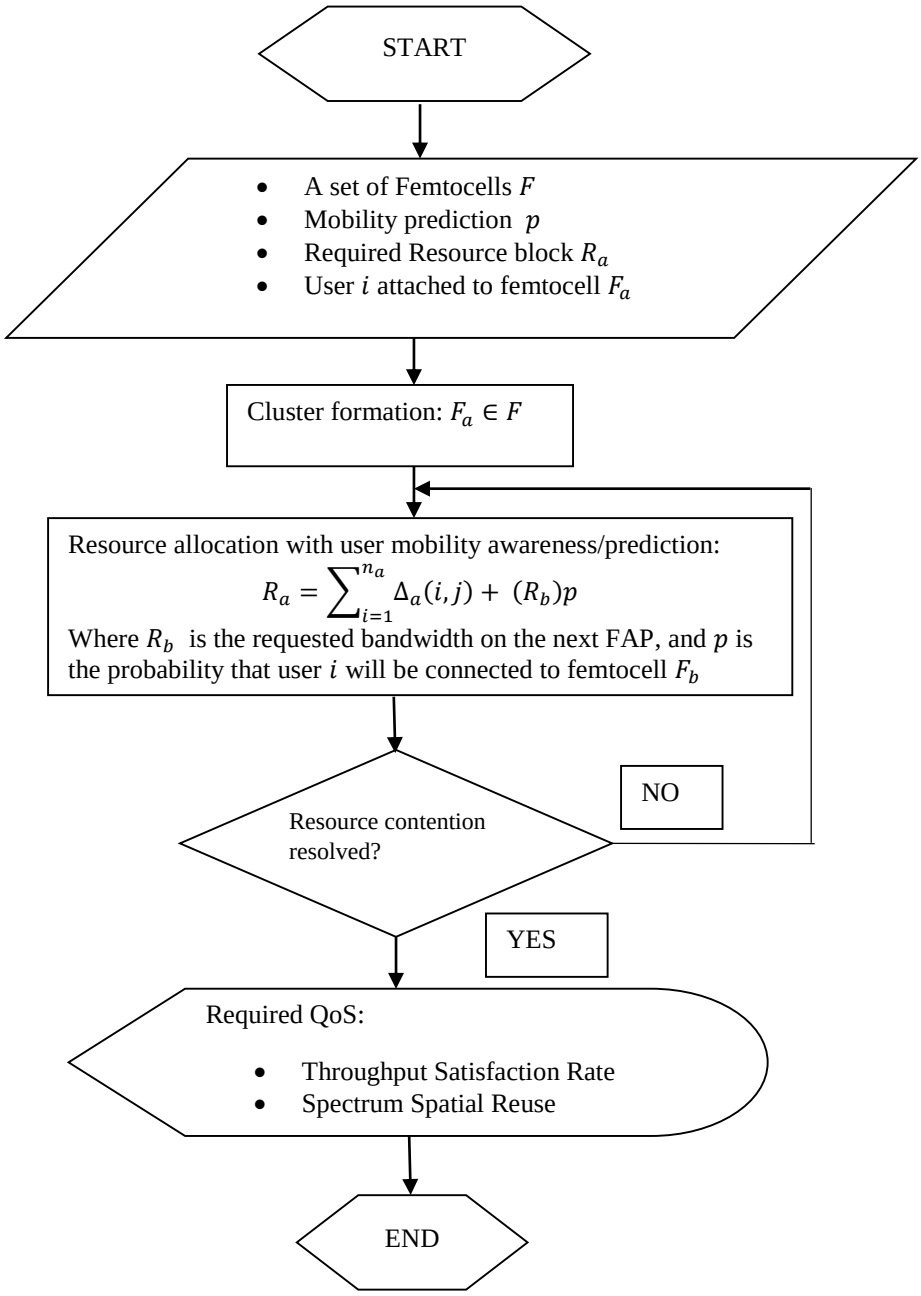

Figure 4.3 M-FCRA Algorithm Flowchart

It optimized the resource allocation under various constrains. LTE-Sim simulator software was used to present simulation results. Simulations were run and the number of mobile nodes attached to each femtocell varied according to set speed of UEs in the network. The analysis was done using a typical OFDMA frame (downlink LTE frame). Mobile users were distributed randomly using random walk algorithm among

femtocells at the start of each simulation and user mobility dynamics incorporated by varying user position with time. Impact of user mobility on the evaluated metrics was analysed.

FCRA algorithm analysed QoS metrics in the study of resource allocation in femtocells network [69]. Considering FCRA as the benchmark to which the potential benefits of M-FCRA have been compared, QoS metrics are analysed for effective validation of the research findings. The QoS metrics analysed in M-FCRA are: Throughput Satisfaction Rate (TSR) and Spectrum Spatial Reuse (SSR).

The system was designed and solution to the mathematical min-max optimization problem solved by mixed integer linear programming method using the solver "ILOG CPLEX".

As described in section 4.2, M-FCRA problem is formulated and users' mobility dynamics incorporation as denoted by:

$$R_a = \sum_{i=1}^{n_a} \Delta_a(i,j) + (R_b)p \tag{4.6}$$

where n_a is the total number of users belonging to femtocell F_a and R_b is the reserved tiles in the next FAP user i to be connected. Total number of required tiles R_a is not constant and depends on the arrival/departure process of end users [69]. The maximum feasible tiles allocation to femtocell F_a is denoted by W_a. In addition for each femtocell $F_a \in F$, a variable $G_a(F_a)$ was defined, which represents the gap between the required and allocated resources of femtocell F_a while considering mobile user mobility trace from stage t to stage $(t+1)$. That is:

$$G_a(F_a) = \left(\frac{W_a - \sum_{i=1}^{n_a} \sum_{j=i}^{T} \Delta_a(i,j)}{R_a} \right) \tag{4.7}$$

where T is the total number of available resources (tiles) for F_a to allocate within a finite time horizon. The main objective of M-FCRA is to minimize the maximum gap between the allocated and the required tiles with user mobility considered. Hence the

maximum value of $G_a(F_a)$ is minimized given the set of interferer femtocells $I_a, \forall F_a \in F$ and for every epoch δ_t. As such, a certain degree of fairness was guaranteed among all users as shown in the simulation results. The min-max optimization problem was formulated as shown:

$$min[max\ G_a(F_a)] \qquad \forall F_a \in F \tag{4.8}$$

$Subject\ to$:

(a) $\forall F_a \in F$: $\sum_{i,j} \Delta_a(i,j) \leq R_a$

(b) $\forall i,j, \forall F_a \in F, \forall F_b \in I_a$: $\Delta_a(i,j) + \Delta_b(i,j) \leq 1$

(c) $\forall i,j, \quad \forall F_a \in F$: $P(i), \Delta_a(i,j) \in \{0,1\}$

(d) $\forall i,j, \quad \forall F_a \in F$: $P(i) \in \{P_e, P_m\}$

Condition (a) denotes that the resource scheduler must guarantee that femtocells cannot obtain more than the required spectrum. Inequality (b) ensures that two interfering femtocells cannot use the same tiles. Condition (c) indicates that $P(i)$ and $\Delta.(j)$ are binary variables and (d) denotes that $P(i)$ is either equal to P_e or P_m.

Mobility of users was introduced by considering the predictive probability of a user leaving one femtocell to another. Every user in the network provided information concerning the neighbouring femtocells and the probability of joining any by solving GPA or LPA. The information as mentioned earlier characterised by requested bandwidth at each stage t was used by CH to reserve resources at stage $t + 1$ which are to be allocated once that user is handed over. FAP at stage t then decides to reallocate the resources left at its disposal.

The resource allocation problem was a multi-objective optimization problem and had been proved to be NP-hard [74]. To solve it, the problem was subdivided into sub-problems by means of clustering. This approach drastically reduced the time complexity of the resource allocation problem and implies successive provisioning steps as described in the next section.

4.5 PERFORMANCE METRICS

The performance of M-FCRA was evaluated considering the following QoS metrics: Throughput Satisfaction Rate and Spectrum Spatial Reuse

4.5.1 Throughput Satisfaction Rate (TSR)

TSR denotes the degree of satisfaction of a user with respect to the requested resources. For each user i attached to a FAP $F_a \in F$, $TSR(i)$ is defined as the ratio of the allocated number of tiles to the requested ones and can be expressed as follows:

$$\forall i, \qquad TSR(i) = \left(\sum_{j=i}^{T} \Delta_{.}^{i}(j) \right) / D_{.}^{i} \tag{4.9}$$

For a network with n_a users, the TSR metric was thus given by:

$$TSR = \sum_{i} TSR(i)/n_a \tag{4.10}$$

4.5.2 Spectrum Spatial Reuse (SSR)

SSR denotes the average portion of FAPs using the same tile within the network. Therefore, it is defined as the mean value of tiles' spatial reuse. The SSR metric can be thus expressed as follows:

$$SSR = \frac{1}{M \times |F|} \sum_{k=1}^{T} \sum_{i=1}^{n_a} \Delta_a(i) \tag{4.11}$$

4.6 METHODOLOGY AND SIMULATION TOOLS

To evaluate the approach in section 4.4, the system described in Chapter 4 is simulated using an open source C++ framework network simulator LTE-Sim [89]. The Min-Max resource allocation optimization problem are solved by the linear programming (LP) solving software, ILOG CPLEX [75], using the ILOG Concert Technology. The optimization programming language CPLEX code is listed in Appendix B.

LTE-Sim is an open source framework to simulate LTE networks. The developed LTE Simulator, LTE-Sim, encompasses several aspects of LTE networks, including both the Evolved Universal Terrestrial Radio Access (E-UTRAN) and the Evolved Packet System (EPS). It supports single and heterogeneous multi-cell environments, QoS management, multi-users environment, user mobility, handover procedures, and frequency reuse techniques. Four kinds of network nodes are modeled: user equipment (UE), evolved Node B (eNB), Home eNB (HeNB), and Mobility Management Entity/Gateway (MME/GW). Four different traffic generators at the application layer have been implemented and the management of data radio bearer is supported. Finally, well-known scheduling strategies (such as Proportional Fair, Modified Largest Weighted Delay First, and Exponential Proportional Fair, Log and Exp rules), AMC scheme, Channel Quality Indicator feedback, frequency reuse techniques, and models for physical layer have been developed [89]. LTE-Sim mobility code is presented in Appendix C.

4.7 SINR ANALYSIS

In this part of the chapter, signal to interference and noise ratio (SINR) and QoS encountered by UEs in femtocell network are analysed.

Each UE attached to its associated femtocell which is responsible for providing service for this UE. Each UE is interfered with by all neighbouring femtocells operating on the same frequency sub-bands like its serving FAP.

The downlink SINR for any UE was calculated using equation 4.12 below.

$$SINR_{UE} = \frac{P_R^{F_a}}{\sigma^2 + \sum_{I_a=1}^{F-1} P_R^{I_a}} \tag{4.12}$$

Where;

P_R^{Fa} is the received power from the serving femtocell F_a

σ^2 is the thermal noise power in Watts

F total number of femtocells in the network

I_a interfering femtocell

The received power P_R was directly calculated using equation 5.2 below.

$$P_R(dBm) = P_F(dBm) - P_{TL}(dB) \tag{4.13}$$

Where;

P_F is the femtocell transmission power in dBm

P_{TL} is the total loss encountered by the signal in dB such that;

$$P_{TL}(dB) = P_L(dB) - G_T(dB) \tag{4.14}$$

Where;

P_L is the path loss encountered by the signal in dB

G_T is the transmitting antenna gain in dB. The receiver antenna gain G_R is set to 0 dB since the UEs antenna pattern set to be omnidirectional. Results and discussion of the simulations are presented next.

CHAPTER FIVE

5.0 RESULTS AND DISCUSSIONS

This chapter provides the simulation results from the M-FCRA approach. Moreover, the simulation methodology used in this thesis is explained and different system and simulation parameters for the studied scenario are presented.

5.1 SIMULATION RESULTS

Figures 5.1 – 5.7 illustrate the single cell with femtocells scenario and simulation results. This work considered a scenario with randomly and uniformly distributed user equipment and femtocells respectively as shown in Figure 5.1.

Distance in metres along Y-axis and X-axis indicate position of the building with respect to overlying macrocell. The femtocells are inside a building where macrocell coverage is poor. At the beginning of simulation, each FAP has 2 users attached to it.

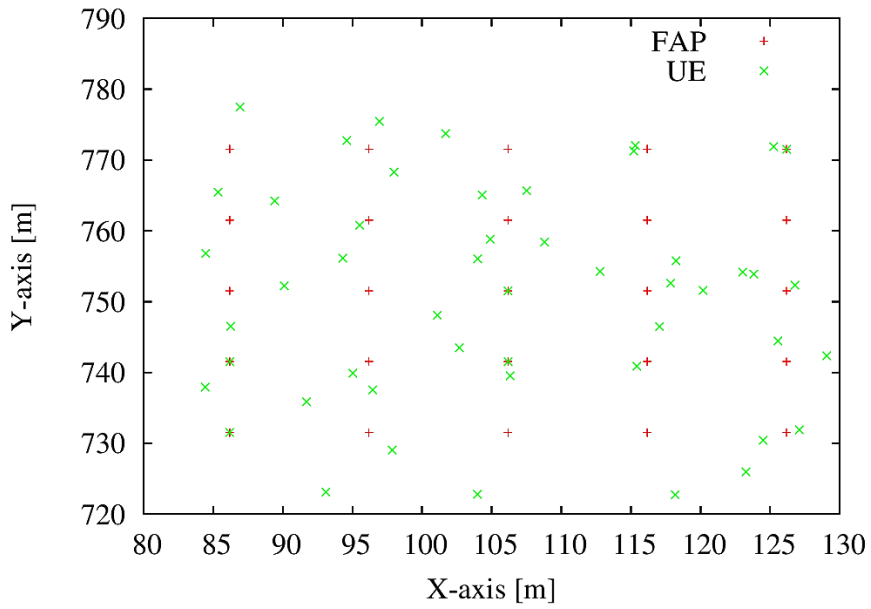

Figure 5.1 Random distribution of users and uniform distribution of FAPs

FCRA scheme considered UEs as static while M-FCRA scheme with UEs moving at 3 km/h in the simulations. Figure 5.2 shows the approximate trajectory of each mobile user in the network after 60 seconds. The direction of the users are random in the building. As illustrated, some users walk out of while others walk into the building.

The average throughput satisfaction rate against time was plotted as shown in Figure 5.3. It improves for M-FCRA and remains constant for FCRA. In the case of users moving closer to the FAPs they are connected, path loss reduces and hence SINR increases. This improves the SINR for the M-FCRA scheme, thus better throughput on higher SINR.

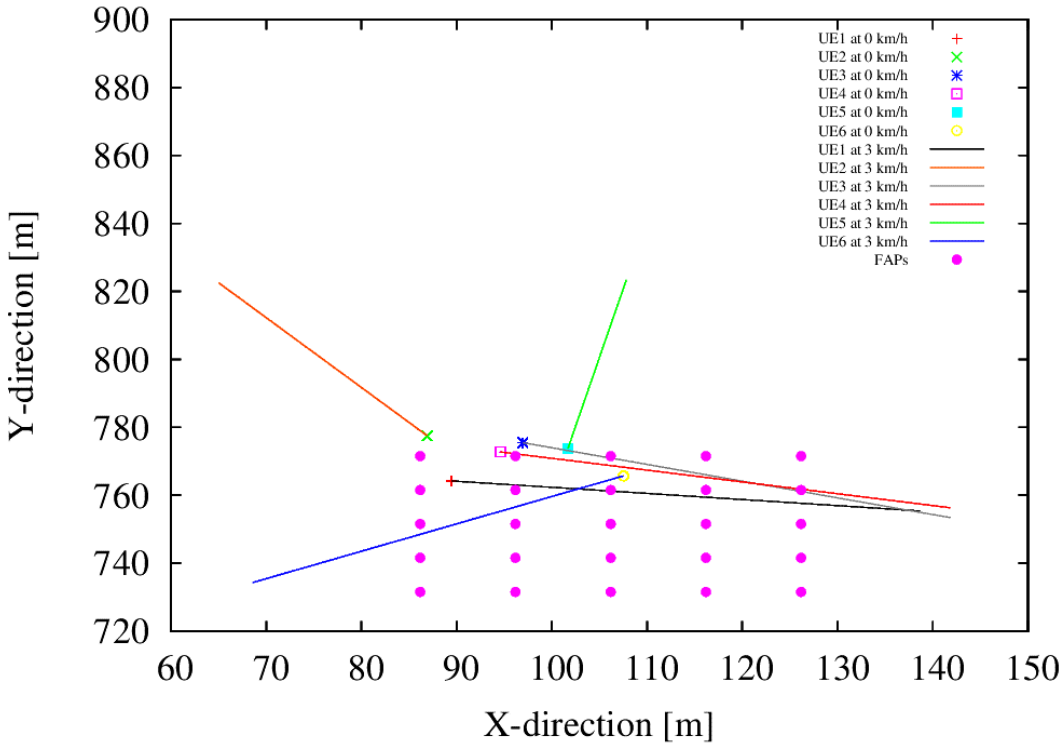

Figure 5.2 Trajectory of some users

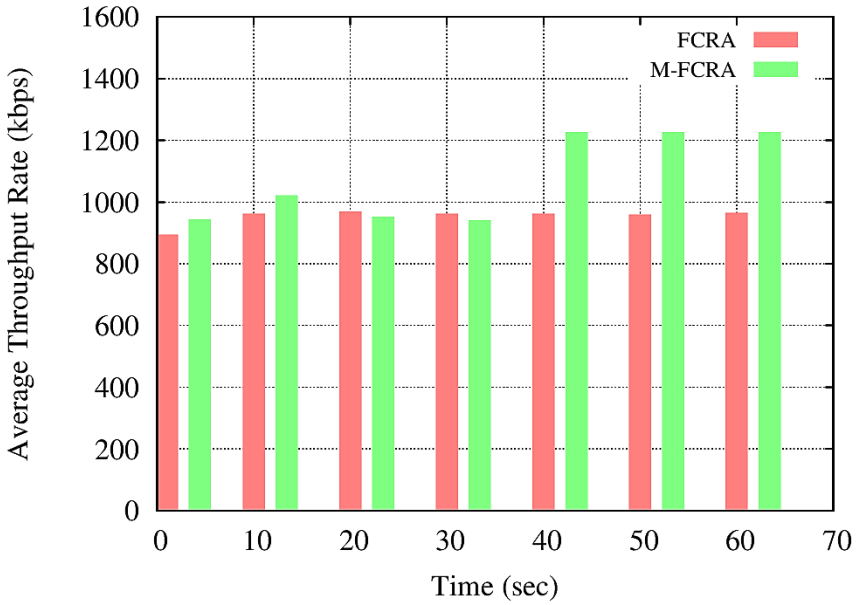

Figure 5.3 Average throughput rate as a function of time.

Since users under FCRA are static, its SINR largely remains constant therefore its average throughput with time remains almost the same. After 30 seconds of connections, M-FCRA outperforms FRCA by about 35%. Consequently, users get better quality of service on M-FCRA scheme.

Figure 5.4 shows average throughput taken per FAP within 60 seconds. The graph indicates that FAPs at the centre of the building performed better in terms of average throughput rate on M-CRA than those at the edge i.e 1, 2 and 22, 23, 24 and 25. This was attributed to low mobility at the edges and handovers of users leaving the building. M-FCRA scheme outperforms FCRA due to reduced path loss hence improved SINR. However, FCRA performs better on the edge FAPs than M-FCRA since users are static and therefore FAPs kept traffic.

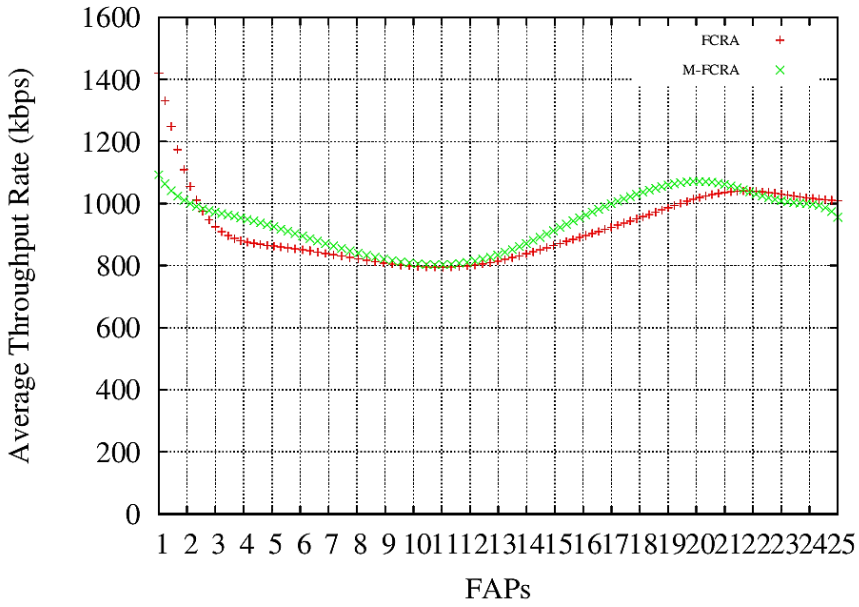

Figure 5.4 Average throughput of each FAP.

The plot of maximum throughput with SINR is illustrated in Figure 5.5. As the SINR improves, throughput rate increases. This is because of reduced path loss in M-FCRA due to mobility of users as opposed to FCRA. M-FCRA achieves SINR up to 40 dB while the best for FCRA is about 28 dB.

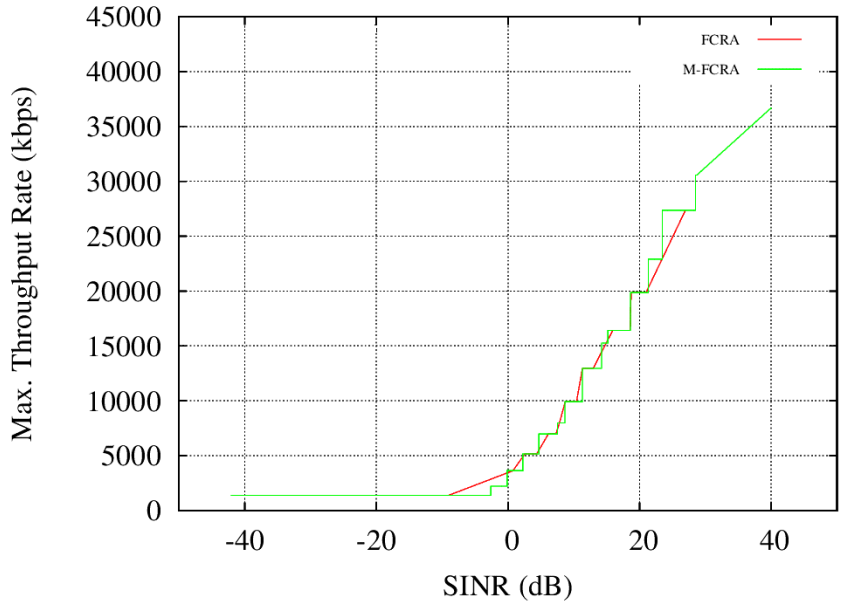

Figure 5.5 Maximum throughput rate per SINR

In Figure 5.6, the spectrum spatial reuse (SSR) of M-FCRA and FCRA schemes as a function of SINR was plotted. Two main observations were made. First, FCRA offers a constant SSR value. At convergence the SINR for FCRA scheme is constant because users are static.

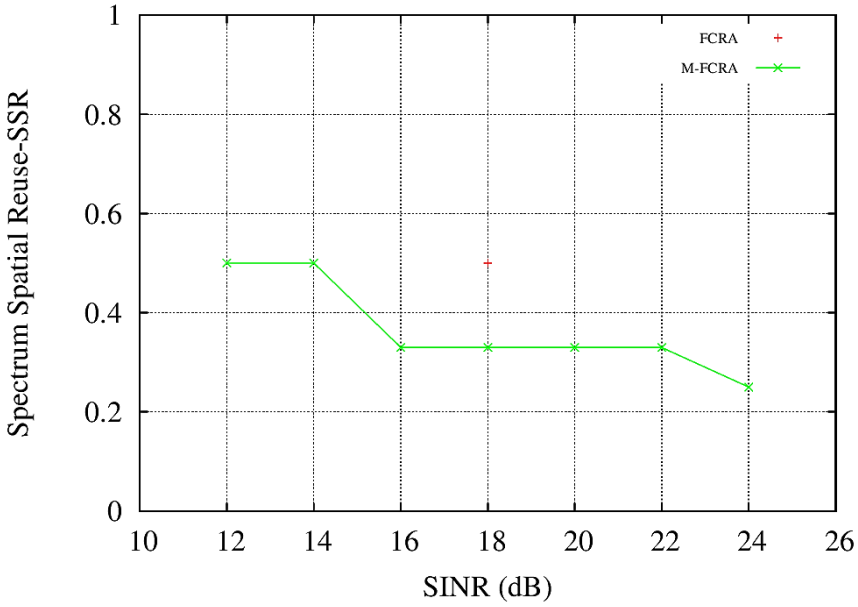

Figure 5.6 Spectrum Spatial Reuse vs SINR.

The network service on a constant SSR at each and every value of SINR as sent to FAPs by users. Second, SSR metric decreases with the increase of SINR for M-FCRA since there is decrease of interference level of each femtocell. This graph considers one user both at static position and while mobile. According to M-FCRA approach, a fewer but densely populated clusters are created. Subsequently, the possibility of reutilization of the same RB (tile) among the formed clusters is decreased. M-FCRA does not allow reutilization of the same resource block/tile within the same cluster.

The degree of interference in the network is inversely proportional to the number of allocated tiles. This is illustrated in Figure 5.7. As SINR increases, the number of tiles allocated to each FAP increases exponentially. This shows that mobile users enjoy better quality of service on average as opposed to static users at poor or low SINR. Static users cannot improve SINR since they cannot move closer to serving FAP.

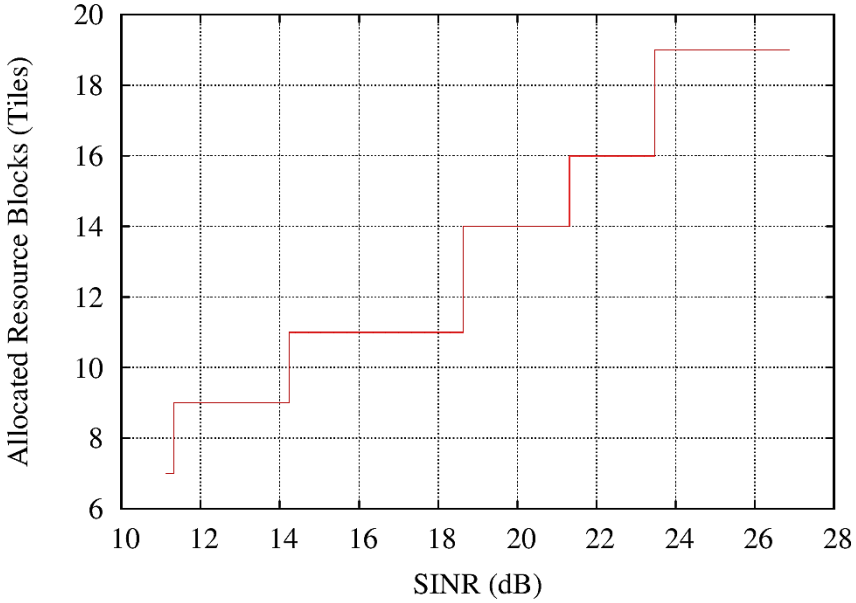

Figure 5.7 Allocated resource blocks vs SINR

5.2 VALIDATION OF RESULTS

In this section, the efficiency of M-FCRA is evaluated under various interference scenarios. FCRA [18] scheme was used as benchmark to which the M-FCRA potential benefits are compared. The reported results were obtained using the solver "IBM ilog cplex" [75] and network simulator "LTE-Sim simulator" [89]. The number of users in each FAP and their position with time varied during the simulation period. A typical OFDMA frame (downlink LTE frame) consisting of M = 50 tiles is considered. In the simulator, femtocell is represented by geometric properties and it is used for detailing the position and the ID of a femtocell. The building is composed of a number of apartments, each one delimiting the area of a given femtocell.

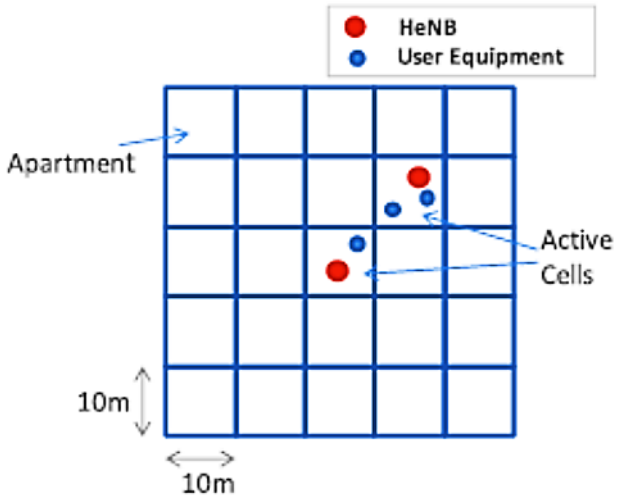

Figure 5.8 A 5 × 5 Apartment Grid

As defined in [17] a 5 × 5 apartment grid is considered as in Figure 5.8. The building is composed of 25 apartments which are located over a 5 × 5 grid. A unique ID is used to identify each building and its position is defined by a Cartesian system. Each squared form apartment has an area of 100m^2. Generally, each apartment contains at least one active FAP, that is, an active Home Evolved Node B (HeNB) in each femtocell. For instance, a 5 × 5 grid building can contain up to 25 femtocells active HeNB. The probability that an active home base station is present in an apartment can be randomly decided through the definition of an activity ratio [90]. Activity ratio is the ratio of active to inactive femtocells in the building at any given time.

This scenario models a single cell with a number of overlapping femtocells. The number of femtocells per building is equal to 25 and the total number of femtocells in the scenario is equal to 25xNumber of Buildings. The parameters used are listed in Table 5.1

The simulator logs all events to the standard output according to the debug level set to study a certain performance criteria. In addition, the log file provides the Cartesian position of all cells and UEs, the channels allocated to each eNB, as well as the unique ID that each UE and eNB is assigned [91]. A large log file is generated and the output is directed to a file and post-processing is done via grep, sed and awk to filter and print relevant performance metrics.

A sample of simulator output is: TX INF_BUF ID 104 B 14 SIZE 290 SRC 0 DST 5 T 1.709. This logs a transmission event for an infinite buffer source with packet ID 104 for bearer 14. The packet size is 290 bytes and source is node 0 and destination is 5. The event occurs at time 1.709 sec. Similarly, a receive event is logged as follows: RX INF_BUF ID 106 B 14 SIZE 290 SRC -1 DST 5 D 0.001 as listed in Appendix D and E for static and mobile users respectively.

Table 5-1 Parameters Used

Parameter	**Value**
Cell Radius	1 km
Number of Buildings	1
Building Type	5 × 5 apartment grid
Activity Ratio	1
Number of Macrocell UE	0
Number of Femtocell UE	2 to 6
Traffic	VIDEO and VoIP
Scheduling Type	Proportional Fair
Frame Structure	FDD
Bandwidth	10 MHz
Speed	0 km/h for FCRA 3 km/h for M-FCRA
Access Policy	Open
MaxDelay	0.1 sec
Video Bit Rate	128 kbps

A 25 FAPs network was considered, representing a small-sized networks. The FAPs were distributed uniformly in a 2-D 50 M × 50 M area, with one FAP randomly placed in a 10 M × 10 M room. Note that some of the residences might not have a FAP or the FAP might be switched off. A 5 × 5 building residence blocks was considered. This basically represents a neighbourhood. Users were randomly distributed within the residence with a maximum number of 6 users per FAP. Each user uniformly generates its traffic demand that can be directly translated to a certain number of tiles using the Equation (a), with a maximum value of 10 tiles per user. Different minimum required SINR thresholds: 10, 15, 20 and 25 dB were considered to show the impact of the interference level on the evaluated metrics. Based on the SINR, the path loss

model given in the A1 scenario for indoor small office and residential of WINNER [73] for the frequency range 2-6 GHz, each femtocell determines the set of its interfering femtocells depending on the received signal strength. It is worth noting that each SINR threshold corresponds to a certain MCS. For example and according to [92], 16 QAM modulation with a coding rate of 3/4 corresponds to a minimum SINR threshold between 10 and 15 dB. While higher order of MCS (e.g., 64 QAM 3/4 or 64 QAM 5/6) requires, respectively, a threshold of 17.5 dB and 20 dB.

CHAPTER SIX

6.0 CONCLUSION AND FUTURE WORK

6.1 CONCLUSION

In this thesis, incorporation of users' mobility dynamics awareness in resource allocation algorithm in femtocell network to enable resource reservation by predicting the next FAP for connection was investigated. The resource allocation problem has been formulated and validated mathematically as a min-max optimization problem. The mathematical problem has been solved using mixed linear integer programming in ILOG CPLEX solver. The simulation scenario developed using LTE-Sim simulator and results were presented.

The performance results from the M-FCRA approach show that incorporation of user mobility dynamics in resource allocation algorithm improves overall user throughput irrespective of users' position with time within femtocell network. This can be attributed to the fact that SINR gains are significant hence better throughput.

In addition, the capacity and quality of service improvement in the network are of benefit to operators in terms of offloading macrocell traffic hence low operating expenditures. Users enjoy uninterrupted traffic indoors under mobility.

The general conclusion which can be drawn from the given results is that incorporation of users' mobility dynamics in resource allocation algorithm is an efficient means to improve network reliability and QoS in indoor femtocell network. As mentioned in this work, more data traffic originate from indoor and hence a lot of interest with emerging technologies are focused in this area.

6.2 FUTURE WORK

To accomplish more comprehensive performance evaluation of resource allocation algorithms in OFDMA femtocell networks, the following future works are suggested:

- Power allocation: As mentioned in the literature, power and subcarrier form very important part of efficient spectrum utilization, the first step for further research could address dynamic power allocation instead of resource blocks in OFDMA femtocells.

- Shared spectrum: Instead of split spectrum as assumed in this work, a shared spectrum can also be studied to evaluate the performance of M-FCRA in OFDMA femtocell networks.
- An algorithm on Collision – Avoidance of Allocated Resources with Neighbouring Clusters.

REFERENCES

[1] International Telecommunication Union, “The World in 2014 ICT Facts and Figures,” ITU, Switzerland, Geneva, 2014.

[2] 3GPP, “Tech. Specif. Group Radio Access Network - Requirements for Evolved UTRA (E-UTRA) and Evolved UTRAN (E-UTRAN), 3GPP TS 25.913”.

[3] International Telecommunication Union (ITU), “Overall network operation, telephone service, service operation and human factors,” ITU-R Recommendations E.800 Annex B, 2008.

[4] F. Tariq, *Interference Aware Cognitive Femtocell Networks,* The Open University, 2012.

[5] K. Juha, Introduction to 3G Mobile Communication, 2 ed., Boston, London: Artech House, 2003.

[6] L. H. Per, “Telenor,” 2000.

[7] H. Atarashi, A. Hashimoto, and H. Yoshino, “Roadmap of IMT-Advanced development,” *IEEE Microwave Magazine*, vol. 9, no. 4, pp. 80-88, 2008.

[8] S. Liu, J. Wu, C. Ha Koh and V. K. N. Lau, “A 25Gb/s(Km2) urban wireless network beyond IMT-advanced,” *IEEE Communications Magazine,* vol. 49, no. 2, pp. 122-129, 2011.

[9] ABI Research, Feb. 5 2011. [Online]. Available: http://www.cellular-news.com/story/33163.php. [Accessed 5 Dec 2014].

[10] M. M. R. Chowdhury, M. B. Ahmad, A. K. Ayaz and J. Noll, “On the Impact of Indoor Data Traffic in Mobile Networks,” in *Wireless World Research Forum*, Kingston, UK, 2010.

[11] The Broadband Commission, “The state of Broadband 2013 - Universalizing Broadband,” ITU, 2013.

[12] C. V. G. M. D. T. F. U. 2013-2018, “Cisco,” Cisco, 5 Feb 2014. [Online]. Available: www.cisco.com. [Accessed 10 Dec 2014].

[13] 4G Americas, “Mobile Broadband Explosion - The 3GPP Wireless Evolution,” Rysavy Research, 2012.

[14] J. Perez-Romero, O. Sallent, and R. Agusti, “Impact of Indoor Traffic W-CDMA Capacity,” in *PIMRC, 15th IEEE International Symposium*, Barcelona, Spain, 2004.

[15] C. E. Shannon, “Communication in the Presence of Noise,” in *Instit. of Radio*, 1998.

[16] S. Sesia, T. Issam and B. Mathew, LTE, The UMTS Long Term Evolution: From Theory to Practice, John Wiley & Sons, 2011.

[17] F. Capozzi, G. Piro, L. A. Grieco, G. Boggia and P. Camarda, “On accurate simulations of LTE femtocells using an open source simulator,” *EURASIP Journal on Wireless Communication and Networking,* 2012.

[18] 3GPP, “Tech. Specif. Group Radio Access Network - Physical Channel Modulation (Release 8), 3GPP TS 36.211”.

[19] Anritsu, “LTE Resource Giude,” 2009.

[20] R. K. Preet, M. S. L. Mohit and A. Rahul, “White Paper on Throughput Calculation for LTE TDD and FDD Systems,” 2012.

[21] K. Farooq, LTE for 4G Mobile Broadband, An Air Interface Technologies and Performance, New York City: Cambridge University Press, 2009, p. 3.

[22] R. W. Chang,, “Synthesis of band-limited orthogonal signals for multichannel data transmission,” *Bell Systems Technical Journal,* vol. 45, pp. 1775-1796, 1966.

[23] R. B. Saltzberg, “Performance of an efficient parallel data transmission system,” *IEEE Transactions on Communications,* Vols. COM-15, no. 6, pp. 805-811, 1967.

[24] S. Ahmad, “WPA Too!,” in *Defcon18,* 2011.

[25] G. A. Jeffrey, C. Holger, D. Mischa, R. Sundeep and R. C. Mark, “Femtocells: Past, Present and Future,” *IEEE Journal on Selected Areas in Communications,* vol. 30, no. 3, p. 497508, 2012.

[26] K. Venceslav, “Femtocell: A solution for Fixed Mobile Convergence - Presentation,” in *ICT Forum Meeting*, Masit Macedonia, 2010.

[27] C. Y. Wong, R. S. Cheng, K. B. Letaief, and R. D. Murch, “Multiuser OFDM with adaptive subcarrier, bit, and power allocation,” *IEEE Journal on Selected Areas in Communications,* vol. 17, no. 10, pp. 1747-1758, 1999.

[28] W. Rhee and J. M. Cioffi, “Increase in capacity of Multiuser OFDM system using dynamic subchannel allocation,” in *IEEE Vehicular Technology Conference VTC*, 2000.

[29] I. Kim, H. L. Lee, B. Kim, and Y. H. Lee, “On the use of linear programming for dynamic subchannel and bit allocation in multiuser OFDM,” in *IEEE Globecom 2001*, 2001.

[30] D. Kivanc, G. Li, and H. Lui, “Computationally efficient bandwidth allocation and power control for OFDMA,” *IEEE Transactions on Wireless Communications,* vol. 2, no. 6, pp. 1150-1158, 2003.

[31] G. Song and Y. Li, “Cross-layer optimization for OFDM wireless networks - Part I,” *IEEE Transactions on Wireless Communications,* vol. 4, no. 2, pp. 614-624, 2005.

[32] G. Song and Y. Li, “Cross-layer optimization for OFDM wireless networks - Part II,” *IEEE Transactions on Wireless Communications,* vol. 4, no. 2, pp. 625-634, 2005.

[33] I. C. Wong, Zukang Shen, B. L. Evans, and J. G. Andrews, “A low complexity algorithm for proportional resource allocation in OFDMA systems,” in *IEEE Workshop on Signal Processing Systems (SIPS)*, 2004.

[34] J. Jang and L. B. Kwang, “Transmit power adaptation for multiuser OFDM systems,” *IEEE Journal on Selected Areas in Communications,* vol. 21, pp. 171-178, 2003.

[35] G. Munz, S. Pfletschinger, and J. Speidel, “An efficient waterfilling algorithm for multiple access OFDM,” in *IEEE Global Telecommunications Conference (GLOBECOM '02)*, 2002.

[36] K. Kim Y. Han, and S. Kim, “Joint subcarrier and power allocation in uplink OFDMA systems,” *IEEE Communications Letters,* vol. 9, no. 6, pp. 526-528, 2005.

[37] M. Shen, G. Li, and L. Hui, “Design tradeoffs in OFDMA traffic channels,” in *IEEE International Conference on Acoustics, Speech, and Signal Processing (ICASSP '04),* 2004.

[38] S. J. Honade and P. V. Ingole, “Removal of Multiple Access Interference in DS-CDMA System,” *International Journal of Scientific and Research Publications,* vol. 2, no. 6, pp. 1-6, 2012.

[39] S. Das, H. Viswanathan, and G. Rittenhouse, “Dynamic load balancing through coordinated scheduling in packet data systems,” in *IEEE INFOM,* 2003.

[40] Y. I. Min, J. H. Jang and H. J. Choi, “Power control scheme for effective serving cell selection in relay environment of 3GPP LTE-Advanced System,” in *J. KICS,* 2011.

[41] A. Sang, X. Wang, M. Madihian, and R. D. Gitlin, “Coordinated load balancing, handoff/cell-site selection, and scheduling in multi-cell packet data systems,” in *ACM MobiCom,* 2004.

[42] H. Lee, “Optimal Cell Selection Scheme for Load Balancing in Heterogeneous Radio Access Networks,” *J. KICS,* vol. 37B, no. 12, 2012.

[43] F. Qian, Z. Wang, A. Gerber, Z. M. Mao, S. Sen, and O. Spatscheck, “Characterizing radio resource allocation for 3G networks,” in *Proc. IMC'10*, 2010.

[44] K. Sandaresan and S. Rangarajan, “Efficient resource management in ofdma femtocells,” *International Symposium on Mobile Ad Hoc Networks and Computing (Mobihoc),* 2009.

[45] J.-H. Yun, and K. G. Shin, “CTRL: a self-organizing femtocell management architecture for co-channel deployment,” in *Proc. ACM MobiCom,* 2010.

[46] Y. Bejerano, and S.-J. Han, “Cell breathing techniques for load balancing in wireless LANs,” in *IEEE Trans. Mobile Comput,* 2009.

[47] O. Ekici and A. Yongacoglu, “A novel association algorithm for congestion relief in IEEE 802.11 WLANs,” in *Proc. IWCMC*, 2006.

[48] H. Velayos, V. Aleo, and G. Karlsson, “Load balancing in overlapping wireless LAN cells,” in *Proc. IEEE ICC*, 2004.

[49] A. J. Nicholson, and B. D. Noble, “Breadcrumbs: forecasting mobile connectivity,” in *Proc. ACM MobiCom*, 2008.

[50] A. Balasubramanian, R. Mahajan, and A. Venkataramani, “Augmenting mobile 3G using WiFi,” in *Proc. ACM MobiSys*, 2010.

[51] M.-R. Ra, J. Paek, A. B. Sharma, R. Govindan, M. H. Krieger, and M. J. Neely, “Energy-delay tradeoffs in smartphone applications,” in *Proc. ACM MobiSys*, 2010.

[52] A. Schulman, et al, “Bartendr: a practical approach to energy-aware cellular data scheduling,” in *Proc. ACM MobiCom*, 2010.

[53] X. Jing, S. S. Anandaraman, M. A. Ergin, I. Seskar, and D. Raychaudhuri,, “Distributed coordination schemes for multi-radio co-existence in dense spectrum environments: an experimental study on the ORBIT testbed,” in *Proc. IEEE Symposium*, 2008.

[54] K. Piamrat, A. Ksentini, J.-M. Bonnin, and C. Viho, “Radio resource management in emerging heterogeneous wireless networks,” *Comput. Commun*, vol. 34, no. 9, pp. 1066-1076, 2011.

[55] W. Song, W. Zhuang, and Y. Cheng, “Load balancing for celluar/WLAN integrated networks,” *IEEE Network*, vol. 21, no. 1, pp. 27-33, 2007.

[56] L. Gao, X. Wang, G. Sun, and Y. Xu, “A game approach for cell selection and resource allocation in heterogeneous wireless networks,” in *Proc. IEEE SECON*, 2011.

[57] M. Gerla and J. T. Tsai, “Multicluster, mobile, multimedia radio network,” *Wireless Networks*, vol. 1, 1995.

[58] N. H. Vaidya, P. Krishna, M. Chatterjee and D. K. Pradhan, “A cluster-based approach for routing in dynamic networks,” *ACM Computer Communications Review,* vol. 27, no. 2, 1997.

[59] C. R. Lin and M. Gerla, “Adaptive clustering for mobile wireless networks,” *IEEE Journal on Selected Areas in Communications,* vol. 15, no. 7, 1997.

[60] R. Ramanathan and M. Steenstrup, “Hierarchically-organized, multihop mobile wireless networks for quality-of-service support,” *Mobile Networks and Applications,* no. 3, 1998.

[61] A. B. McDonald and T. F. Znati, “A mobility-based framework for adaptive clustering in wireless ad hoc networks,” *IEEE Journal on Selected Areas in Communications,* vol. 17, no. 8, 1999.

[62] S. Basagni, “Distributed clustering for ad-hoc networks,” *in Proceedings of ACM ISPAN,* pp. 310-315, 1999.

[63] A. Antis, R. Prakash, T. Voung, and D. Huynh, “Max-Min d-cluster formation in wireless ad-hoc networks,” *IEEE INFOCOM,* 2000.

[64] S. Banerjee and S. Khuller, “A clustering scheme for hierarchical control in multi-hop wireless networks,” *IEEE INFOCOM,* 2001.

[65] Y. Chen and A. Liestman, “Approximating minimum size weakly-connected dominating sets for clustering mobile ad-hoc networks,” *in Proceedings of ACM MobiHoc,* pp. 165-172, 2002.

[66] O. Younis and S. Fahmy, “Distributed clustering in ad-hoc sensor networks: A hybrid, energy-efficient approach,” *in Proceedings of IEEE INFOCOM,* pp. 624-640, 2004.

[67] B. Aoun, R. Boutaba, Y. Iraqi and G. Kenward, “Gateway placement optimization in wireless mesh networks with QoS constraints,” *IEEE Journal on Selected Areas in Communications (JSAC), Special Issue on Multi-hop wireless Mesh Networks,* vol. 24, pp. 2127-2136, 2006.

[68] N. Bouabdallah, R. Langar, and R. Bontaba, “Design and analysis of mobility-aware clustering algorithms for wireless mesh networks,” *IEEE/ACM Transactions on Networking,* vol. 18, no. 6, pp. 1677-1690, 2010.

[69] A. Hatoum, A. Nadjib, L. Rami, B. Raouf and P. Guy, “FCRA: Femtocell Cluster-based Resource Allocation Scheme for OFDMA Networks,” *IEEE International Conference on Communication,* 2011.

[70] L. G. U. Garcia, K. I. Pedersen, and P. E. Mogensen, “Autonomous component carrier selection: Interference management in local area environment for lte-advanced,” *IEEE Communication Magazine,* vol. 47, 2009.

[71] V. Chandrasekhar and J. Andrews, “Spectrum allocation in tiered cellularnetworks,” *IEEE Transaction on Communications,* 2009.

[72] D. Lopez-Perez, A. Valcarce, G. de la Roche, and J. Zhang, “Ofdma femtocells: A roadmap on interference avoidance,” *IEEE Communication Magazine,* 2009.

[73] D. WINNER II, “Winner II channel models part I - channel models,” Tech. Rep, 2007.

[74] H. Aissi, C. Bazgan, and D. Vanderpooten, “Complexity of the min-max and min-max regret assignment problems,” *Operation Research Letters,* 2005.

[75] IBM, “http://www.ilog.com/products/cplex/”.

[76] 3GPP, “3GPP Tech. Spec. Rep. 36.921 version 10.0.0 release 10”.

[77] S. Leei, “An enhanced IEEE 1588 time synchronizition algorithm for asymmetric communication link using block burst transmission,” *IEEE Comm. Lett.,* vol. 12, no. 9, 2008.

[78] A. Hatoum, L. Rami, A. Nadjib and P. Guy, “Q-FCRA: QoS-based OFDMA Femtocell Resource Allocation Algorithm,” *IEEE,* pp. 5151-5156, 2012.

[79] I. Guvenc, M. -R. Jeong, F. Watanabe, and H. Inamura, “Hybrid frequency assignment for femtocells and coverage area analysis for cochannel operation,” *IEEE Comm. Lett.,* 2008.

[80] V. Chandrasekhar and J. Andrews, “Power control in two-tier femtocell networks,” *IEEE Trans. on Wireless Communications,* 2009.

[81] N. Chakchouk and B. Hamdaoui, “Uplink performance characterization and analysis of two-tier femtocell networks,” *IEEE Trans. Veh. Tech.,* vol. 61, no. 9, 2012.

[82] 3GPP, "3GPP Tech. Spec. TS 36.300 v 10.5.0, Evolved Universal Terrestrial Radio Access (E-UTRA) and Evolved Universal Terrestrial Radio Access Network (E-UTRAN); Overall Description; stage 2," 2011.

[83] A. Hatoum, R. Langar, A. Nadjib, B. Raouf and P. Guy, "Cluster-based Resource Management in OFDMA Femtocell Networks with QoS Guarantees," *IEEE Transactions on Vehicular Technology,* 2013.

[84] Y. Arslan, J. Yoon, K. Sundaresan, V. Krishnamurthy, and S. Banerjee, "A femtocell resource management system for interference mitigation in OFDMA networks," in *International Conference on Mobile Computing and Networking (MobiCom),* 2011.

[85] Y. -H. Liang et al, "Resource allocation with interfeence avoidance in OFDMA femtocell networks," *IEEE Trans. Veh. Tech,* vol. 61, no. 5, 2012.

[86] B. Dominique, C. Amira, L. Kloul and M. Oliver, "Femtocells Sharing Management using Mobility Prediction Model," in *16th ACM international conference on Modeling, analysis & simulation of wireless and mobile systems*, ACM New York, NY, USA, 2013.

[87] S. Bellahsene and L. Kloul, "A new markov-based mobility prediction algorithm for mobile networks," Bertinoro Italy, 2010.

[88] S. Bellahsene, L. Kloul, and D. Barth, "A hierarchical prediction model for two nodes-based ip mobile networks," in *12th MSWiM,* Canary Islands, Spain, 2009.

[89] telematics, "http://telematics.poliba.it/index.php/en/lte-sim".

[90] 3GPP, "Simulation Assumptions and Parameters for FDD HenB RF requirements, 3GPP TSG RAN TS 36.331," 3GPP, 2009.

[91] 4G++, "Advanced Performance Boosting Techniques in 4th Generation Wireless System," (online).

[92] A. Ladanyi, D. Lopez-Perez, A. Jutter, X. Chuy, and J. Zhang, "Distributed resource allocation for femtocell interference coordination via power minimization," in *IEEE GLOBECOM*, 2011.

APPENDICES

Appendix 1 Published Work

1. Nicholas O. Oyie, Philip K. Langat, S. Musyoki "Bandwidth Allocation Algorithm with User Mobility Dynamics in Femtocell Network," *Communications*, vol. 3, pp 8-17, 2014
2. Nicholas O. Oyie, Philip K. Langat, S. Musyoki "A Mobility-aware Resource Allocation Scheme for Femtocell Networks," in *Proc. 8th JKUAT Scientific, Technological and Industrialization Conference*, Nov 14-15, 2013, pp 1088-1096
3. Nicholas O. Oyie, Philip K. Langat, S. Musyoki "Resource Allocation Optimization in Femtocell Networks: IBM ILOG CPLEX," in *Proc. 8th Egerton University International Conference*, March 26-28, 2014, 744-753
4. Nicholas O. Oyie, Philip K. Langat, S. Musyoki "Femtocell Cluster-based Mobility-aware Resource Allocation Scheme for OFDMA Networks" in *Proc. JKUAT Sustainable Research and Innovation Conference*, May 7-9, 2014, pp 247-250.

Appendix 2 Min-Max Optimization OPL CPLEX Code

```
/*********************************************
 * OPL 12.6.0.0 Model
 * Author: Admin
 * Creation Date: 19 Aug 2014 at 12:49:45
 *********************************************/
int Femtos = 10;
int NbUsers = 2;
int NbTiles = 20;

assert(NbTiles>=NbUsers);

range Users = 1..NbUsers;
range Tiles = 1..NbTiles;

int Capacity [u in Users] = NbTiles div Femtos;
int RBW [t in Tiles][u in Users] = (t*u);

dvar int CUsers[Users] in 0..1;
dvar int UTiles[Tiles][Users] in 0..1;

dexpr float TotalBWUsed = max(u in Users, t in Tiles) RBW[t][u]-
sum(u in Users, t in Tiles) CUsers[u]*UTiles[t][u]-sum(u in Users,
t in Tiles) CUsers[u]*UTiles[t][u];
dexpr float TotalRBW = max(u in Users, t in Tiles) RBW[t][u];
dexpr float Obj = TotalBWUsed - TotalRBW;

minimize Obj;

subject to {
forall(t in Tiles, u in Users)
  sum(u in Users)
    UTiles[t][u] <= RBW[t][u];
    forall(u in Users)
      sum(t in Tiles)
        UTiles[t][u]>= CUsers[u]*Capacity[u];
}
```

Appendix 3 LTE-Sim Mobility Code

```
#include "Mobility.h"
#include "../componentManagers/NetworkManager.h"
#include "../networkTopology/Cell.h"
#include "../load-parameters.h"

Mobility::Mobility()
{
  m_AbsolutePosition = NULL;
}

Mobility::~Mobility()
{
  delete m_AbsolutePosition;
}

void
Mobility::SetNodeID (int id)
{
  m_nodeID = id;
}

int
Mobility::GetNodeID (void) const
{
  return m_nodeID;
}

void
Mobility::SetMobilityModel(MobilityModel model)
{
  m_mobilityModel = model;
}

Mobility::MobilityModel
Mobility::GetMobilityModel(void) const
{
  return m_mobilityModel;
}

void
Mobility::SetAbsolutePosition (CartesianCoordinates *position)
{
  if (position == NULL)
    {
            m_AbsolutePosition = NULL;
      return;
    }

  if (m_AbsolutePosition == NULL)
```

```
   {
          m_AbsolutePosition = new CartesianCoordinates ();
   }

 m_AbsolutePosition->SetCoordinateX (position->GetCoordinateX ());
 m_AbsolutePosition->SetCoordinateY (position->GetCoordinateY ());
}

CartesianCoordinates*
Mobility::GetAbsolutePosition (void) const
{
 return m_AbsolutePosition;
}

void
Mobility::DeleteAbsolutePosition (void)
{
 delete  m_AbsolutePosition;
}

void
Mobility::SetSpeed (int speed)
{
 m_speed = speed;
}

int
Mobility::GetSpeed (void) const
{
 return m_speed;
}

void
Mobility::SetSpeedDirection (double speedDirection)
{
 m_speedDirection = speedDirection;
}

double
Mobility::GetSpeedDirection (void) const
{
 return m_speedDirection;
}

void
Mobility::SetPositionLastUpdate (double time)
{
 m_positionLastUpdate = time;
}

double
```

```
Mobility::GetPositionLastUpdate (void) const
{
  return m_positionLastUpdate;
}

void
Mobility::SetHandover (bool handover)
{
  m_handover = handover;
}

bool
Mobility::GetHandover (void) const
{
  return m_handover;
}

void
Mobility::SetLastHandoverTime (double lastHOtime)
{
  m_handoverLastRun = lastHOtime;
}

double
Mobility::GetLastHandoverTime (void) const
{
  return m_handoverLastRun;
}

double
Mobility::GetTopologyBorder (void)
{
  int nbCell = NetworkManager::Init()->GetNbCell();

  switch (nbCell)
    {
      case 1:
            return (NetworkManager::Init()->GetCellByID (0)->GetRadius () * 1000);
            break;
      case 7:
            return ((2.6 * NetworkManager::Init()->GetCellByID (0)->GetRadius ()) * 1000);
            break;
      case 19:
          return ((4. * NetworkManager::Init()->GetCellByID (0)->GetRadius ()) * 1000);
          break;
      default:
            return 1000.0;
            break;
    }
}
```

Appendix 4 LTE-Sim Data for FCRA (speed at 0km/h)

Created Building, id 0, position: 106.178 751.537 and 1 floors and 25 femtocells
Created enb, id 0, cell id 0, position: 0 0, channels id 00
BandwidthManager: 0x2faba70
operative sub band: 1
m_dlBandwidth 10
m_ulBandwidth 10
m_dlOffsetBw 0
m_ulOffsetBw 0
DL channels: 2110 2110.18 2110.36 2110.54 2110.72 2110.9 2111.08 2111.26 2111.44 2111.62 2111.8 2111.98 2112.16 2112.34 2112.52 2112.7 2112.88 2113.06 2113.24 2113.42 2113.6 2113.78 2113.96 2114.14 2114.32 2114.5 2114.68 2114.86 2115.04 2115.22 2115.4 2115.58 2115.76 2115.94 2116.12 2116.3 2116.48 2116.66 2116.84 2117.02 2117.2 2117.38 2117.56 2117.74 2117.92 2118.1 2118.28 2118.46 2118.64 2118.82
UL channels: 1920 1920.18 1920.36 1920.54 1920.72 1920.9 1921.08 1921.26 1921.44 1921.62 1921.8 1921.98 1922.16 1922.34 1922.52 1922.7 1922.88 1923.06 1923.24 1923.42 1923.6 1923.78 1923.96 1924.14 1924.32 1924.5 1924.68 1924.86 1925.04 1925.22 1925.4 1925.58 1925.76 1925.94 1926.12 1926.3 1926.48 1926.66 1926.84 1927.02 1927.2 1927.38 1927.56 1927.74 1927.92 1928.1 1928.28 1928.46 1928.64 1928.82
Created Home enb, id 1, cell id 1, position: 86.1777 771.537, channels id 11
BandwidthManager: 0x2faba70
operative sub band: 1
m_dlBandwidth 10
m_ulBandwidth 10
m_dlOffsetBw 0
m_ulOffsetBw 0
DL channels: 2110 2110.18 2110.36 2110.54 2110.72 2110.9 2111.08 2111.26 2111.44 2111.62 2111.8 2111.98 2112.16 2112.34 2112.52 2112.7 2112.88 2113.06 2113.24 2113.42 2113.6 2113.78 2113.96 2114.14 2114.32 2114.5 2114.68 2114.86 2115.04 2115.22 2115.4 2115.58 2115.76 2115.94 2116.12 2116.3 2116.48 2116.66 2116.84 2117.02 2117.2 2117.38 2117.56 2117.74 2117.92 2118.1 2118.28 2118.46 2118.64 2118.82
UL channels: 1920 1920.18 1920.36 1920.54 1920.72 1920.9 1921.08 1921.26 1921.44 1921.62 1921.8 1921.98 1922.16 1922.34 1922.52 1922.7 1922.88 1923.06 1923.24 1923.42 1923.6 1923.78 1923.96 1924.14 1924.32 1924.5 1924.68 1924.86 1925.04 1925.22 1925.4 1925.58 1925.76 1925.94 1926.12 1926.3 1926.48 1926.66 1926.84 1927.02 1927.2 1927.38 1927.56 1927.74 1927.92 1928.1 1928.28 1928.46 1928.64 1928.82
.
.
.
UserPosition X [at 0] 89.4126 86.9133 96.9437 94.5819 101.687 107.513 115.207 115.321 126.178 125.238 85.3496 84.4572 95.5071 97.9939 104.303 104.904 108.808 112.781 123.036 123.822 86.253 90.117 101.083 94.3092 106.178 103.99 117.855 120.177 126.78 118.237 86.1777 84.4164 95.0271 96.447 102.682 106.178 117.049 115.422 129.062 125.557 86.1777 91.6952 97.8486 93.0808 103.981 106.324 123.254 118.18 127.105 124.498
UserPosition Y [at 0] 764.22 777.491 775.463 772.742 773.735 765.687 771.296 772.053 771.537 771.88 765.45 756.842 760.795 768.297 765.07 758.82 758.424 754.294 754.179 753.891 746.537 752.231 748.081 756.174 751.537 756.033 752.625 751.606 752.335 755.773 741.537 737.945 739.901 737.546 743.481 741.537 746.46 740.882 742.363 744.472 731.537 735.844 729.045 723.086 722.809 739.535 725.975 722.762 731.911 730.451

UserPosition X [at 0.001] 89.4126 86.9133 96.9437 94.5819 101.687 107.513 115.207 115.321 126.178 125.238 85.3496 84.4572 95.5071 97.9939 104.303 104.904 108.808 112.781 123.036 123.822 86.253 90.117 101.083 94.3092 106.178 103.99 117.855 120.177 126.78 118.237 86.1777 84.4164 95.0271 96.447 102.682 106.178 117.049 115.422 129.062 125.557 86.1777 91.6952 97.8486 93.0808 103.981 106.324 123.254 118.18 127.105 124.498
UserPosition Y [at 0.001] 764.22 777.491 775.463 772.742 773.735 765.687 771.296 772.053 771.537 771.88 765.45 756.842 760.795 768.297 765.07 758.82 758.424 754.294 754.179 753.891 746.537 752.231 748.081 756.174 751.537 756.033 752.625 751.606 752.335 755.773 741.537 737.945 739.901 737.546 743.481 741.537 746.46 740.882 742.363 744.472 731.537 735.844 729.045 723.086 722.809 739.535 725.975 722.762 731.911 730.451
.
.
.
TX INF_BUF ID 2206990 B 134 SIZE 1490 SRC 23 DST 70 T 59.999 0
TX INF_BUF ID 2206991 B 134 SIZE 536 SRC 23 DST 70 T 59.999 0
TX INF_BUF ID 2206992 B 140 SIZE 1226 SRC 24 DST 72 T 59.999 0
TX INF_BUF ID 2206993 B 149 SIZE 1490 SRC 25 DST 75 T 59.999 1
TX INF_BUF ID 2206994 B 149 SIZE 536 SRC 25 DST 75 T 59.999 1
DL_SINR 26 89.4126 764.22 -13.7747 0 1384
DL_SINR 27 86.9133 777.491 26.9693 24 27376
RX INF_BUF ID 2206960 B 5 SIZE 1490 SRC -1 DST 27 D 0.001 0
RX INF_BUF ID 2206961 B 5 SIZE 1349 SRC -1 DST 27 D 0.001 0
DL_SINR 28 96.9437 775.463 9.59991 12 9912
RX INF_BUF ID 2206962 B 8 SIZE 1226 SRC -1 DST 28 D 0.001 1
DL_SINR 29 94.5819 772.742 17.5754 18 16416
DL_SINR 30 101.687 773.735 4.37721 6 5160
RX INF_BUF ID 2206963 B 14 SIZE 632 SRC -1 DST 30 D 0.001 1
DL_SINR 31 107.513 765.687 -9.73261 0 1384
DL_SINR 32 115.207 771.296 18.3078 18 16416
RX INF_BUF ID 2206964 B 20 SIZE 1490 SRC -1 DST 32 D 0.001 1
RX INF_BUF ID 2206965 B 20 SIZE 392 SRC -1 DST 32 D 0.001 1
.
.
.

TX INF_BUF ID 2206995 B 5 SIZE 1490 SRC 1 DST 27 T 60 0
TX INF_BUF ID 2206996 B 5 SIZE 1349 SRC 1 DST 27 T 60 0
TX INF_BUF ID 2206997 B 11 SIZE 1490 SRC 2 DST 29 T 60 1
TX INF_BUF ID 2206998 B 11 SIZE 392 SRC 2 DST 29 T 60 1
TX INF_BUF ID 2206999 B 14 SIZE 632 SRC 3 DST 30 T 60 1

SIMULATOR_DEBUG: Stop ()

Appendix 5 LTE-Sim Data of M-FCRA (speed at 3km/h)

Created Building, id 0, position: 106.178 751.537 and 1 floors and 25 femtocells
Created enb, id 0, cell id 0, position: 0 0, channels id 00
BandwidthManager: 0x20c4a70
operative sub band: 1
m_dlBandwidth 10
m_ulBandwidth 10
m_dlOffsetBw 0
m_ulOffsetBw 0
DL channels: 2110 2110.18 2110.36 2110.54 2110.72 2110.9 2111.08 2111.26 2111.44 2111.62 2111.8 2111.98 2112.16 2112.34 2112.52 2112.7 2112.88 2113.06 2113.24 2113.42 2113.6 2113.78 2113.96 2114.14 2114.32 2114.5 2114.68 2114.86 2115.04 2115.22 2115.4 2115.58 2115.76 2115.94 2116.12 2116.3 2116.48 2116.66 2116.84 2117.02 2117.2 2117.38 2117.56 2117.74 2117.92 2118.1 2118.28 2118.46 2118.64 2118.82
UL channels: 1920 1920.18 1920.36 1920.54 1920.72 1920.9 1921.08 1921.26 1921.44 1921.62 1921.8 1921.98 1922.16 1922.34 1922.52 1922.7 1922.88 1923.06 1923.24 1923.42 1923.6 1923.78 1923.96 1924.14 1924.32 1924.5 1924.68 1924.86 1925.04 1925.22 1925.4 1925.58 1925.76 1925.94 1926.12 1926.3 1926.48 1926.66 1926.84 1927.02 1927.2 1927.38 1927.56 1927.74 1927.92 1928.1 1928.28 1928.46 1928.64 1928.82
Created Home enb, id 1, cell id 1, position: 86.1777 771.537, channels id 11
BandwidthManager: 0x20c4a70
operative sub band: 1
m_dlBandwidth 10
m_ulBandwidth 10
m_dlOffsetBw 0
m_ulOffsetBw 0
DL channels: 2110 2110.18 2110.36 2110.54 2110.72 2110.9 2111.08 2111.26 2111.44 2111.62 2111.8 2111.98 2112.16 2112.34 2112.52 2112.7 2112.88 2113.06 2113.24 2113.42 2113.6 2113.78 2113.96 2114.14 2114.32 2114.5 2114.68 2114.86 2115.04 2115.22 2115.4 2115.58 2115.76 2115.94 2116.12 2116.3 2116.48 2116.66 2116.84 2117.02 2117.2 2117.38 2117.56 2117.74 2117.92 2118.1 2118.28 2118.46 2118.64 2118.82
UL channels: 1920 1920.18 1920.36 1920.54 1920.72 1920.9 1921.08 1921.26 1921.44 1921.62 1921.8 1921.98 1922.16 1922.34 1922.52 1922.7 1922.88 1923.06 1923.24 1923.42 1923.6 1923.78 1923.96 1924.14 1924.32 1924.5 1924.68 1924.86 1925.04 1925.22 1925.4 1925.58 1925.76 1925.94 1926.12 1926.3 1926.48 1926.66 1926.84 1927.02 1927.2 1927.38 1927.56 1927.74 1927.92 1928.1 1928.28 1928.46 1928.64 1928.82
.
.
.
UserPosition X [at 0] 89.4126 86.9133 96.9437 94.5819 101.687 107.513 115.207 115.321 126.178 125.238 85.3496 84.4572 95.5071 97.9939 104.303 104.904 108.808 112.781 123.036 123.822 86.253 90.117 101.083 94.3092 106.178 103.99 117.855 120.177 126.78 118.237 86.1777 84.4164 95.0271 96.447 102.682 106.178 117.049 115.422 129.062 125.557 86.1777 91.6952 97.8486 93.0808 103.981 106.324 123.254 118.18 127.105 124.498
UserPosition Y [at 0] 764.22 777.491 775.463 772.742 773.735 765.687 771.296 772.053 771.537 771.88 765.45 756.842 760.795 768.297 765.07 758.82 758.424 754.294 754.179 753.891 746.537 752.231 748.081 756.174 751.537 756.033 752.625 751.606 752.335 755.773 741.537 737.945 739.901 737.546 743.481 741.537 746.46 740.882 742.363 744.472 731.537 735.844 729.045 723.086 722.809 739.535 725.975 722.762 731.911 730.451

UserPosition X [at 0.001] 89.4126 86.9133 96.9437 94.5819 101.687 107.513 115.207 115.321 126.178 125.238 85.3496 84.4572 95.5071 97.9939 104.303 104.904 108.808 112.781 123.036 123.822 86.253 90.117 101.083 94.3092 106.178 103.99 117.855 120.177 126.78 118.237 86.1777 84.4164 95.0271 96.447 102.682 106.178 117.049 115.422 129.062 125.557 86.1777 91.6952 97.8486 93.0808 103.981 106.324 123.254 118.18 127.105 124.498
UserPosition Y [at 0.001] 764.22 777.491 775.463 772.742 773.735 765.687 771.296 772.053 771.537 771.88 765.45 756.842 760.795 768.297 765.07 758.82 758.424 754.294 754.179 753.891 746.537 752.231 748.081 756.174 751.537 756.033 752.625 751.606 752.335 755.773 741.537 737.945 739.901 737.546 743.481 741.537 746.46 740.882 742.363 744.472 731.537 735.844 729.045 723.086 722.809 739.535 725.975 722.762 731.911 730.451
.
.
.
UserPosition X [at 59.999] 138.624 65.0416 141.817 141.807 107.816 68.5958 71.5099 123.021 77.6823 174.145 45.4572 118.455 126.307 59.6305 54.3778 86.8833 123.457 142.889 160.097 112.464 36.52 41.2267 148.36 48.6616 57.2874 109.962 108.203 125.282 120.571 105.341 45.2583 35.0456 74.5916 142.062 139.85 112.307 104 153.734 79.1359 114.199 130.329 89.1196 145.912 113.298 131.828 153.828 169.935 95.5276 105.233 119.156
UserPosition Y [at 59.999] 755.385 822.452 753.412 756.322 823.356 734.297 795.594 722.651 783.704 782.27 795.59 720.181 800.18 736.233 767.765 712.183 806.228 794.21 720.62 705.2 741.393 762.699 764.351 776.574 762.005 706.392 703.568 701.869 702.724 804.079 770.267 745.841 694.269 717.074 776.922 791.158 698.195 773.007 745.058 695.78 754.998 785.776 742.82 677.358 681.283 723.941 743.885 767.335 776.872 680.738
TX INF_BUF ID 759963 B 5 SIZE 1226 SRC 1 DST 27 T 59.999 0
TX INF_BUF ID 759964 B 14 SIZE 1226 SRC 3 DST 30 T 59.999 0
TX INF_BUF ID 759965 B 29 SIZE 1226 SRC 5 DST 35 T 59.999 0
TX INF_BUF ID 759966 B 95 SIZE 1226 SRC 16 DST 57 T 59.999 0
RX INF_BUF ID 759964 B 14 SIZE 1226 SRC -1 DST 30 D 0.001 0
.
.
.
.
UserPosition X [at 60] 138.625 65.0412 141.818 141.808 107.817 68.5952 71.5091 123.021 77.6815 174.146 45.4566 118.455 126.308 59.6298 54.377 86.883 123.457 142.89 160.098 112.463 36.5192 41.2259 148.361 48.6608 57.2866 109.962 108.203 125.282 120.571 105.341 45.2576 35.0447 74.5913 142.063 139.851 112.307 104 153.735 79.1351 114.198 130.33 89.1195 145.913 113.298 131.828 153.829 169.936 95.5273 105.233 119.156
UserPosition Y [at 60] 755.385 822.453 753.412 756.322 823.357 734.297 795.595 722.65 783.704 782.27 795.591 720.181 800.181 736.233 767.765 712.182 806.229 794.211 720.619 705.199 741.393 762.699 764.351 776.574 762.005 706.392 703.567 701.869 702.723 804.08 770.267 745.842 694.269 717.074 776.923 791.159 698.194 773.007 745.058 695.78 754.999 785.777 742.82 677.357 681.283 723.941 743.885 767.335 776.872 680.738
TX INF_BUF ID 759969 B 29 SIZE 1226 SRC 5 DST 35 T 60 0
TX INF_BUF ID 759970 B 95 SIZE 1226 SRC 16 DST 57 T 60 0

SIMULATOR_DEBUG: Stop ()